



ESCUELA TÉCNICA SUPERIOR DE INGENIERÍA  
(ICAI)

KAUNAS UNIVERSITY OF TECHNOLOGY  
(KTU)

INGENIERO ELECTRICO

Calculation of six phase squirrel cage  
motor, with implementation in electric  
vehicles

Autor: Luis Miguel Millán Cobo  
Director: Jonas Vanagas



Autorizada la entrega del proyecto del alumno:

**Nombre del Autor**

\_\_\_\_\_

EL DIRECTOR DEL PROYECTO

**Nombre del Director**

Fdo.: ..... Fecha: ..... / ..... / .....

\_\_\_\_\_

V<sup>o</sup> B<sup>o</sup> DEL COORDINADOR DE PROYECTOS

**Nombre del Coordinador**

Fdo.: ..... Fecha: ..... / ..... / .....

## **AUTORIZACIÓN PARA LA DIGITALIZACIÓN, DEPÓSITO Y DIVULGACIÓN EN ACCESO ABIERTO ( RESTRINGIDO) DE DOCUMENTACIÓN**

### **1º. Declaración de la autoría y acreditación de la misma.**

El autor D. Luis Miguel Millán Cobo, como estudiante de la UNIVERSIDAD PONTIFICIA COMILLAS (COMILLAS), **DECLARA**

que es el titular de los derechos de propiedad intelectual, objeto de la presente cesión, en relación con la obra \_\_\_\_\_<sup>1</sup>, que ésta es una obra original, y que ostenta la condición de autor en el sentido que otorga la Ley de Propiedad Intelectual como titular único o cotitular de la obra.

En caso de ser cotitular, el autor (firmante) declara asimismo que cuenta con el consentimiento de los restantes titulares para hacer la presente cesión. En caso de previa cesión a terceros de derechos de explotación de la obra, el autor declara que tiene la oportuna autorización de dichos titulares de derechos a los fines de esta cesión o bien que retiene la facultad de ceder estos derechos en la forma prevista en la presente cesión y así lo acredita.

### **2º. Objeto y fines de la cesión.**

Con el fin de dar la máxima difusión a la obra citada a través del Repositorio institucional de la Universidad y hacer posible su utilización de *forma libre y gratuita ( con las limitaciones que más adelante se detallan)* por todos los usuarios del repositorio y del portal e-ciencia, el autor **CEDE** a la Universidad Pontificia Comillas de forma gratuita y no exclusiva, por el máximo plazo legal y con ámbito universal, los derechos de digitalización, de archivo, de reproducción, de distribución, de comunicación pública, incluido el derecho de puesta a disposición electrónica, tal y como se describen en la Ley de Propiedad Intelectual. El derecho de transformación se cede a los únicos efectos de lo dispuesto en la letra (a) del apartado siguiente.

### **3º. Condiciones de la cesión.**

Sin perjuicio de la titularidad de la obra, que sigue correspondiendo a su autor, la cesión de derechos contemplada en esta licencia, el repositorio institucional podrá:

(a) Transformarla para adaptarla a cualquier tecnología susceptible de incorporarla a internet; realizar adaptaciones para hacer posible la utilización de la obra en formatos electrónicos, así como incorporar

---

<sup>1</sup> Especificar si es una tesis doctoral, proyecto fin de carrera, proyecto fin de Máster o cualquier otro trabajo que deba ser objeto de evaluación académica

metadatos para realizar el registro de la obra e incorporar “marcas de agua” o cualquier otro sistema de seguridad o de protección.

(b) Reproducir la en un soporte digital para su incorporación a una base de datos electrónica, incluyendo el derecho de reproducir y almacenar la obra en servidores, a los efectos de garantizar su seguridad, conservación y preservar el formato. .

(c) Comunicarla y ponerla a disposición del público a través de un archivo abierto institucional, accesible de modo libre y gratuito a través de internet.<sup>2</sup>

(d) Distribuir copias electrónicas de la obra a los usuarios en un soporte digital.<sup>3</sup>

#### **4º. Derechos del autor.**

El autor, en tanto que titular de una obra que cede con carácter no exclusivo a la Universidad por medio de su registro en el Repositorio Institucional tiene derecho a:

a) A que la Universidad identifique claramente su nombre como el autor o propietario de los derechos del documento.

b) Comunicar y dar publicidad a la obra en la versión que ceda y en otras posteriores a través de cualquier medio.

c) Solicitar la retirada de la obra del repositorio por causa justificada. A tal fin deberá ponerse en contacto con el vicerrector/a de investigación ([curiarte@rec.upcomillas.es](mailto:curiarte@rec.upcomillas.es)).

d) Autorizar expresamente a COMILLAS para, en su caso, realizar los trámites necesarios para la obtención del ISBN.

---

<sup>2</sup> En el supuesto de que el autor opte por el acceso restringido, este apartado quedaría redactado en los siguientes términos:

(c) Comunicarla y ponerla a disposición del público a través de un archivo institucional, accesible de modo restringido, en los términos previstos en el Reglamento del Repositorio Institucional

<sup>3</sup> En el supuesto de que el autor opte por el acceso restringido, este apartado quedaría eliminado.

d) Recibir notificación fehaciente de cualquier reclamación que puedan formular terceras personas en relación con la obra y, en particular, de reclamaciones relativas a los derechos de propiedad intelectual sobre ella.

#### **5º. Deberes del autor.**

El autor se compromete a:

a) Garantizar que el compromiso que adquiere mediante el presente escrito no infringe ningún derecho de terceros, ya sean de propiedad industrial, intelectual o cualquier otro.

b) Garantizar que el contenido de las obras no atenta contra los derechos al honor, a la intimidad y a la imagen de terceros.

c) Asumir toda reclamación o responsabilidad, incluyendo las indemnizaciones por daños, que pudieran ejercitarse contra la Universidad por terceros que vieran infringidos sus derechos e intereses a causa de la cesión.

d) Asumir la responsabilidad en el caso de que las instituciones fueran condenadas por infracción de derechos derivada de las obras objeto de la cesión.

#### **6º. Fines y funcionamiento del Repositorio Institucional.**

La obra se pondrá a disposición de los usuarios para que hagan de ella un uso justo y respetuoso con los derechos del autor, según lo permitido por la legislación aplicable, y con fines de estudio, investigación, o cualquier otro fin lícito. Con dicha finalidad, la Universidad asume los siguientes deberes y se reserva las siguientes facultades:

##### a) Deberes del repositorio Institucional:

- La Universidad informará a los usuarios del archivo sobre los usos permitidos, y no garantiza ni asume responsabilidad alguna por otras formas en que los usuarios hagan un uso posterior de las obras no conforme con la legislación vigente. El uso posterior, más allá de la copia privada, requerirá que se cite la fuente y se reconozca la autoría, que no se obtenga beneficio comercial, y que no se realicen obras derivadas.

- La Universidad no revisará el contenido de las obras, que en todo caso permanecerá bajo la responsabilidad exclusiva del autor y no estará obligada a ejercitar acciones legales en nombre del autor en el supuesto de infracciones a derechos de propiedad intelectual derivados del depósito y archivo de las obras. El autor renuncia a cualquier reclamación frente a la Universidad por las formas no ajustadas a la legislación vigente en que los usuarios hagan uso de las obras.

- La Universidad adoptará las medidas necesarias para la preservación de la obra en un futuro.

b) Derechos que se reserva el Repositorio institucional respecto de las obras en él registradas:

- retirar la obra, previa notificación al autor, en supuestos suficientemente justificados, o en caso de reclamaciones de terceros.

Madrid, a ..... de ..... de .....

**ACEPTA**

Fdo.....

## **Aim of the graduation project:**

*The final thesis project represent the final application of the knowledge acquire during the career, being this a reference of the quality of the learning process and the skills learned through the years focusing on many expertise related to engineering and research labs. In this project, I tried to apply my knowledge that I inquired to solve real life problems and face them with reasonable solutions scoping with the actual world.*

*With the chance of the realization of the project in Kaunas University of technology, I pretended to learn and experience a different methodology in another engineering school with the purpose of expanding my experience in my domain and open up to new market thinking.*



## **Summary:**

*The aim of this project, which was developed in collaboration with my tutor, is to fulfill the request for external company specialized in the electrical motors equipment. They were requiring a solution for a new project integrated within a plan developed by several European cities that aims to keep the urban city center free from vehicle pollution. Including provisioning vehicles who should be fast enough to move from supplying points to the customers, with the capacity to develop a torque enough and at the same time, to be able to reach a reasonable speed that make them independent.*

*This project covers a rough vision of the thematic side of electrical vehicles. Firstly throughout understanding the context of nowadays, then the trending goals of companies at the time of developing new devices and models, reaching finally to take special care of the efficiency and the standards of constructive limitation. All of this in order to keep always the economical aspect as a main concern.*

*The project includes as well a limited overlook through the basics of the inductive motor, the advantages of implementation on multi-phase motor in this sector of the industry and the calculations for the first prototype that demands the client with higher features of torque and speed for those vehicles, justifying the six phase motor implementation by the limitation of 80 V batteries.*

*Me gustaría agradecer, como no podía ser de otra forma, a mis padres Luis Miguel y Ana, por haber sido tabla en el mar durante el naufragio y haber remado junto a mi cuando mas lo necesitaba.*

*A mi hermano Fernando, por compartir noches de estudio, risas, lágrimas de impotencia y enseñarme todo lo que puedo y debo aprender de él.*

*A mis abuelos, que se que lo han dado todos por sus nietos en este y en el otro mundo.*

*A mis tíos y primos, por que siempre confiaron en que lo conseguiría.*

*A mis amigos que siguen ahí o que de algún modo han pasado durante alguna etapa de la carrera, les debo los buenos ratos que me han sacado la sonrisa cuando los payasos se daban por vencidos o el abrazo cuando ya no había marcha atrás.*

*A mi tutor de proyecto Jonas, por haber depositado en mi desde el primer día toda la confianza de un viejo amigo y haber aprendido , taza de café en mano, todo lo que los libros no podían enseñarme.*

*Y por último a mis profesores de Icai, especialmente a Santiago Canales y Alberto Carnicero, sin los que sin su ayuda y animo en los momentos decisivos, no estaría aquí.*

# *Memory*

# Index:

<b>Descriptive Memory:</b> .....	<b>20</b>
Introduction.....	20
State of Art.....	21
Present Major Issues .....	22
Motivation and the substantiation of six phase squirrel cage motor:.....	23
Overview of the literature:.....	26
Principal components .....	26
Principle of operation: The Rotating Field and Induced Voltages .....	27
Running Operation .....	29
Equivalent Circuit of the Induction Motor .....	30
Performance Characteristics .....	34
Efficiency .....	39
Motor Design Classes .....	41
Design Trends & Influences .....	43
<i>Energy Efficient Design</i> .....	43
<i>Factors limiting the use of higher efficiency motors</i> .....	43
Standards .....	44
<i>Types of duty</i> .....	46
<i>Insulation</i> .....	47
<i>Protection</i> .....	47
Objectives.....	48
Methodology .....	50
<b>Calculations:</b> .....	<b>51</b>
1.Specifications .....	51
2.Magnetic circuits and windings .....	51
<b>2.1</b> <i>Size of stator and rotor magnetic circuits</i> .....	51
<b>2.2.</b> <i>Stator winding</i> .....	54
<b>2.4.</b> <i>Dimensions of rotor slot, tooth, yoke and winding</i> .....	59

2.5. Calculation of magnetic circuit. Magnetizing current. ....	62
2.6. Motor operating conditions parameters.....	65
3. Magnetic and mechanic losses .....	69
4. Motor parameters and characteristics .....	71
4.1. Parameters of equivalent circuit.....	71
4.2. Start characteristics .....	72
4.1. Operating characteristics .....	74
<b>Conclusions:</b> .....	<b>79</b>
<b>Literature and Bibliography:</b> .....	<b>80</b>
<b>Appendix:</b> .....	<b>83</b>

# Figure Index:

Fig. 1 Evolution of population and vehicles.....	21
Fig. 2 Types of EV .....	22
Fig. 3 Electric propulsion subsystem .....	22
Fig. 4 dual-3-phase motor.....	23
Fig. 5 Changes to output power with a fault on one phase.....	25
Fig. 6 Reduction of stator losses.....	25
Fig. 7 Three-phase induction motor. ....	26
Fig. 8 Exploded view of the cage motor of Fig.7.....	27
Fig. 9 Air gap flux density distribution and signal from PWM. ....	28
Fig. 10 Equivalent circuit of a wound-rotor induction motor at .....	31
Fig. 11 Development of the induction machine equivalent circuit.....	32
Fig. 12 Torque-speed profile at different voltages.....	37
Fig. 13 Torque speed characteristics for varying $R_2$ . ....	38
Fig. 14 Power flow in an induction motor.....	40
Fig. 15 motor classes .....	41
Fig. 16 slot shapes.....	42
Fig. 17 class motor table.....	42
Fig. 18 efficiency table.....	45
Fig. 19 Efficiency graph .....	45
Fig. 20 Motor standards specifications .....	46
Fig. 21 Types of duty.....	46
Fig. 22 Types of insulation .....	47
Fig. 23 Types of protection “a” .....	47
Fig. 24 Types of protection “b” .....	48
Fig. 25 V/F curve .....	49
Fig. 26 Stator trapezoid dimensions.....	57
Fig. 27 Stator tooth dimension .....	57
Fig. 28 Stator slot dimensions.....	57
Fig. 29 Rotor trapezoid dimensions .....	60
Fig. 30 Rotor slot dimensions .....	60
Fig. 31 Equivalent circuit parameters.....	71
Fig. 32 equivalent circuit transformation.....	72



## Reference table for parameters:

Name	Definition	Numeration
$h$	Height rotation axis	1
$D_{j1}$	External diameter stator	2
$k_D$	Ratio stator diameters	3
$D_1$	Stator internal diameter	4
$\delta$	Air gap	5
$D_{j2}$	External rotor diameter	6
$k_E$	Factor $k_E$	7
$\eta$	Efficiency	8
$\cos\Phi$	Power factor	9
$P'_1$	Design Power	10
$n_1$	Rotation speed of stator field	11
$k_z$	Mena saturation factor of tooth zone	12
$\alpha_\delta$	Pole arc Factor	13
$k_b$	Field shape factor	14
$B_\delta$	Air gap flux density	15
$A_1$	Stator linear load	16
	Stator winding and slot	17
$q_1$	Number of stator slots per pole and phase	18
$k_{w1}$	Stator winding factor	19
$l_\delta$	Design length of stator magnetic circuit	20
$\lambda_1$	Geometrical dimensions ratio	21
$k_v$	Factor $k_v$	22
$D_2$	Internal diameter of rotor	23
$Z_1$	Number stator slots	24
$\beta$	Relative winding span	25
$Y_{n1}$	Stator winding span	26
$I_{1N}$	Stator winding current	27
$t_1$	Stator slots pitch	28
$N_{n1}$	Effective number of conductors in stator slot	29
$J_1$	Stator winding current density	30
$q$	Cross section area non isolated conductor	31
$J_1$	Actual current density of stator windings	32
$w_1$	Number of stator winding phase serial turn	33
$A_1$	Actual linear load of stator	34
$A1J1$	Winding thermal characteristic	35
$k_{d01}$	Stator winding distribution factor	36
$k_{\beta 1}$	Stator winding span decrease factor	37
$k_{w1}$	Stator winding factor	38
$\Phi_\delta$	Motor air gap magnetic flux	39



$\tau$	Pole pitch	40
$B_{\delta}$	Actual motor air gap magnetic flux	41
	Stator slots	42
	Trapezoid dimensions	43
$B_{j1}$	Stator yoke magnetic flux density	44
$B_{z1}$	Stator tooth magnetic flux density	45
$h_{j1}$	Stator yoke height	46
$b_{z1}$	Stator tooth width	47
	Stator slot dimensions	48
$\Delta b_s, \Delta h_s$	Stator slot dimension tolerance	49
$Q_{n1}$	Stator slot cross section area stamp	50
$Q'_{n1}$	Cross section assembled stator magnetic circuit	51
	Insulation of stator winding slot	52
$b_i$	Thickness of stator slot insulation	53
$Q_i$	Cross section area of stator slot insulation	54
$Q_t$	Cross section area of stator slot streak and closing insulation	55
$Q_{n1f}$	Cross section area of winding stator slots	56
$N_{n1}$	Filling factor of stator slot $k_{cu1}$	57
$t_{1vid}$	Mean pitch of stator slots	58
$b_{ar1}$	Mean area of stator winding coil	59
$L_{s1}$	Mean estimated length of stator winding overheat	60
$L_{ar1}$	Mean length of stator turn	61
$h_{g1}$	Height of stator winding overhand	62
$Z_2$	Rotor slot number	63
	Rotor slot	64
$t_2$	Pitch of rotor slots	65
	Trapezoid dimensions	66
$h_{n2}$	Rotor slot height	67
$B_{z2}$	Rotor tooth magnetic flux density	68
$b_{z2}$	Rotor tooth width	69
$h_{s2}$	Rotor slot dimensions	70
$h_{j2}$	Design height of rotor yoke	71
$B_{j2}$	Magnetic flux density of rotor yoke	72
$q_{cr}$	Cross section area of rotor squirrel cage winding bar	73
$I_c$	Current of rotor squirrel cage winding bar	74
$J_c$	Current density of rotor squirrel cage bar	75
	Rotor slot skewing	76
	Rotor cage ring dimensions	77
$I_z$	Current rotor cage ring	78
$J_z$	Current density of rotor cage ring	79
$k_{n1}$	Factor evaluating dentation of stator	80
$k_{n2}$	Factor evaluating dentation of rotor	81
$k_{\delta}$	Air gap factor	82
$F_{\delta}$	Magnetic potential difference of pole pair air gap	83

$H_{z1}$	Magnetic field strength of stator teeth	84
$L_{z1}$	Design length of stator teeth magnetic lines	85
$F_{z1}$	Magnetic potential difference of stator teeth	86
$L_{z2}$	Design length of rotor teeth magnetic lines	87
$H_{z2}$	Magnetic field strength of rotor teeth	88
$F_{z2}$	Magnetic potential difference of rotor teeth	89
$k_z$	Saturation factor of tooth zone	90
$k_a$	Factor of magnetic flux density change	91
	Corrected values of magnetic fluxes	92
$L_{j1}$	Design length of stator yoke magnetic lines	93
$H_{j1}$	Stator yoke magnetic field strength	94
$F_{j1}$	Stator yoke magnetic potential difference	95
$L_{j2}$	Design length of rotor yoke magnetic lines	96
$H_{j2}$	Rotor yoke magnetic field strength	97
$F_{j2}$	Rotor yoke magnetic potential difference	98
$F_{\Sigma}$	Pole pair magneto motive force	99
$k_s$	Saturation factor of magnetic circuit	100
$I_m$	Magnetizing current	101
$\gamma_{\theta}$	Specific electrical conductance of stator winding	102
$R_1$	Resistance of stator winding phase	103
$\gamma'_{\theta}$	Specific electrical conductance of rotor cage winding	104
$R_c$	Resistance of rotor cage bar	105
$R_z$	Resistance of rotor cage ring part between next bars	106
$R_2$	Resistance of rotor cage winding phase	107
$k_{r1}$	Factor of rotor winding parameters reduction	108
$R'_2$	Reduced resistance of rotor winding phase	109
$k_{\beta}, k'_{\beta}$	Factors	110
$h_1$	Winding height in the slot	111
$\lambda_{n1}$	Relative leakage magnetic conductance of stator slot	112
$k_{d1}$	Factor $k_{d1}$	113
$k_{s1}$	Factor $k_{s1}$	114
$k'_{d1}$	Factor of stator differential leakage	115
$\lambda_{d1}$	Relative magnetic conductance of differential leakage	116
$\lambda_{s1}$	Relative magnetic conductance of stator winding overhand leakage	117
$\Lambda_1$	Relative magnetic conductance of stator winding leakage	118
$X_1$	Reactance of stator winding phase	119
$\lambda_{n2}$	Relative magnetic conductance of rotor slot leakage	120
$k'_{d2}$	Factor of rotor differential leakage	121
$\lambda_{d2}$	Relative magnetic conductance of rotor differential leakage	122
$\lambda_z$	Relative magnetic conductance of rotor cage rings leakage	123
$\Lambda_2$	Relative magnetic conductance of rotor winding leakage	124
$X_2$	Reactance of cage rotor winding phase leakage	125
$X'_2$	Reduced resistance of rotor winding phase leakage	126
$X_m$	Mutual reactance(neglecting diagonal of slots)	127

$\gamma_s$	Central angle of diagonal	128
	Factor	129
$k_{is}$	Factor evaluating diagonals of slots	130
	Leakage reactances when diagonal is accounted	131
$G_{z1}$	Stator teeth mass	132
$G_{j1}$	Stator yoke mass	133
$p_{z1}$	The main magnetic losses of stator teeth	134
$p_{j1}$	The main stator yoke losses	135
$p_{Feh}$	The main magnetic losses	136
$\beta_0$	Factor $\beta_0$	137
$B_0$	Magnitude of magnetic flux density oscillation	138
$p_{s2}$	Specific losses of rotor surface	139
$P_{s2}$	Surface losses of rotor teeth	140
	Rotor teeth mass	141
$\gamma_1$	Factor $\gamma_1$	142
	Magnitude of magnetic flux density oscillation	143
$P_{p2}$	Pulsing losses of rotor teeth	144
$p_{Fea}$	Additional magnetic losses	145
$p_{Fe\Sigma}$	Idle operation magnetic losses	146
$k_m$	Factor $k_m$	147
$P_{m\Sigma}$	Mechanic losses	148
$R_m$	Steel resistance	149
$\gamma_1$	Angle $\gamma_1$	150
$c_1$	Factor $c_1$	151
	Parameters of equivalent circuit	152
$M_m$	Motor maximum torque	153
$s_m$	Motor critical slip $s_m$	154
$a$	Factor $a$	155
$M_p$	Motor start torque	156
$M_N$	Motor dedicated torque	157
$m_m$	Motor relative maximum torque $m_m$	158
$m_p$	Motor relative start torque	159
	Motor mechanic characteristic	160
	Mechanical characteristic according to Kloss equation	161
	Motor operating characteristics and dedicated parameters	162

# Descriptive Memory:

---

## Introduction

Nowadays in the era of telecommunication and electronics, speaking about electric vehicles it is becoming, slowly but with confident steps, in a reality to the majority of the world thank to the daily implementation and inversion of companies in the development and improvement of them. However, until to 1970s, with the people's concern of the air quality and greenhouse effect, the study of electric vehicles became a very trendy topic. Since 1990s, a lot of large vehicle groups and companies, such as FORD, GM, NISSAN, TOYOTA, HONDA, etc. invested larger funds in electric vehicles, and developed a variety of electric vehicles.

The power-driven system of electric vehicle is the tie between energy storage system and the wheels, its role is to change the energy (chemical energy, electrical energy) output by energy storage system to mechanical energy, to promote the vehicles to overcome rolling resistance, air resistance, acceleration resistance and climbing resistance, and to convert kinetic energy to electrical energy feedback to energy storage systems during braking. There are some differences between modern electric vehicles and conventional fuel vehicles, the power drive systems of modern electric vehicles can eliminate the complex and heavy mechanical gear speed change mechanism, providing to meet the torque-speed characteristic.

Motor is the drive unit of electric vehicle, and its technical performance can directly impact on the power and economy of vehicle, so it needs computer-aided to design, analyze electromagnetic field, temperature field and stress field, select and design the electric vehicle which is consistent with the operational requirements of the motor, and it has the features of wide speed adjustable range, large starting torque, high stand-by power, high efficiency, large power density and high reliability.

The selection of the motors of electric vehicles generally includes two main types of multi-phase induction AC motor and permanent magnet DC motor. The DC motor has larger dead weight and poorer maintenance, while induction AC has the features of reliable, simple maintenance, cheap, high efficient, higher specific power and large change of power factor, so it is widely used in the current electric vehicle manufacturing industry.

The aim of this project, which was developed in collaboration with my tutor, is to fulfill the request for external company specialized in the electrical motors equipment. They were requiring a solution for a new project integrated in a plan developed by several European cities which aims to keep the urban city center free from vehicle pollution, including provisioning vehicles. This project covers the calculations for the first prototype that demands the client with higher features of torque and speed for those vehicles, justifying the six phase motor implementation by the limitation of 80 V batteries.

## State of Art

Let us begin with the investigation of the growth of population and vehicles, as shown in Fig. 1. In the next 50 years, the global population will increase from 6 billion to 10 billion and the number of vehicles will increase from 700 million to 2.5 billion. If all these vehicles are propelled by internal combustion engines, can we answer the following questions: There is going to be enough oil? Where the emissions should be disseminated? Would our health be in risk? The gloomy answers to these questions compel people to strive for sustainable road transportation for the 21st century.

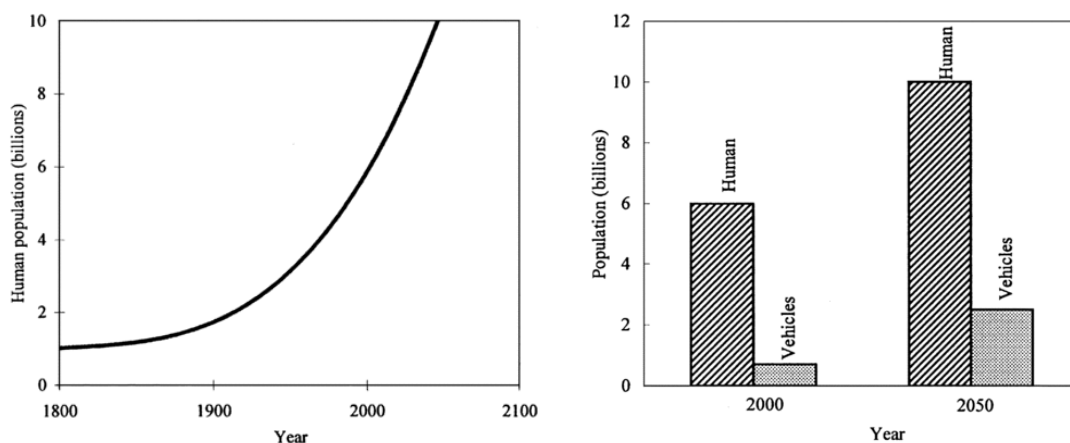


*Fig. 1 Evolution of population and vehicles*

In a world where environmental protection and energy conservation are growing concerns, the development of EV (electrical vehicles) technology has taken on an accelerated pace to fulfill these needs. Concerning the environment, EVs can provide emission-free urban transportation. Even taking into account the emissions from the power plants needed to fuel the vehicles, the use of EVs can still significantly reduce global air pollution. From the energy aspect, EVs can offer a secure, comprehensive, and balanced energy option that is efficient and environmental friendliness, such as the utilization of various kinds of the renewable energies. Therefore, EVs will have the potential to have a great impact on energy, environment and transportation as well as hi-tech promotion, new industry creation, and economic development.

## Different types of hybrid and electric vehicles

Feature	Start/Stop	Micro Hybrid	Mild Hybrid	Full Hybrid (Parallel)	Full Hybrid (Serial)	Full Electric
Start/stop alternator	✓	✓	✓	✓		
Regenerative braking		✓	✓	✓	✓	✓
Electric torque assist			✓	✓		
Electric and combustion drive				✓		
Only electric drive possible					✓	✓
Plug-in capability				✓	✓	✓

Fig. 2 Types of EV

### Present Major Issues

At present, the major driving force for EVs is the environment issue, such as the mandate of EU for 2020 about reducing CO<sub>2</sub> emissions in tripulated and transport vehicles. Thus, the main question to be answered becomes “Can EVs be made affordable?” The major factors that make EV affordable are the range and cost. To tackle the range, the development of advanced batteries such as nickel-metal hydride (Ni-MH), zinc/air (Zn/Air), and lithium-ion (Li-Ion) are in progress. However, since both specific energy and energy density of batteries are much lower than that of gasoline, the development of fuel cells (FCs) for EVs has taken on an accelerated pace in recent years. Meanwhile, the development of commercial HEVs is also going on rapidly. HEVs essentially improve the range and performance of EVs at higher complexity and cost because of the additional energy source, engine, and other accessories. To tackle the cost, efforts are being made to improve various EV subsystems, such as electric motors, power converters, electronic controllers, energy management units, battery chargers, batteries, and other EV auxiliaries, as well as EV system-level integration and optimization.

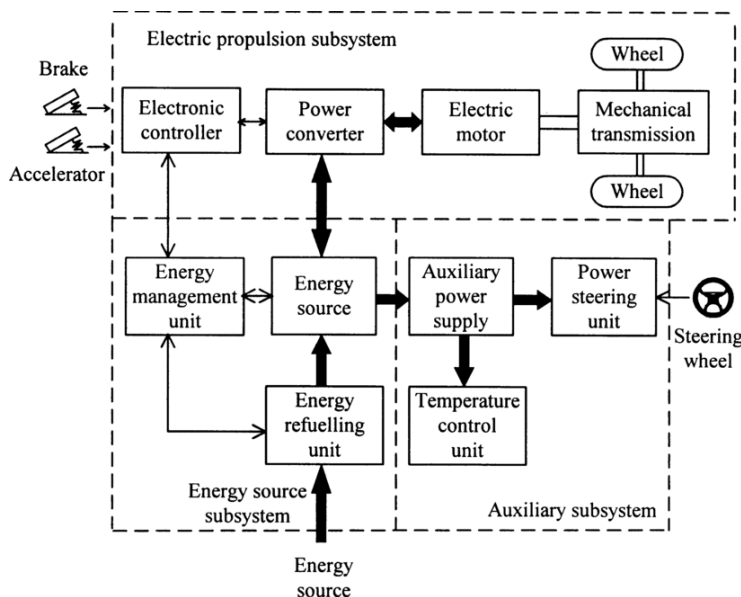


Fig. 3 Electric propulsion subsystem

Amongst many types of electrical motors, induction motors still enjoy the same popularity as they did a century ago. Several factors which include robustness, low cost and low maintenance have made them popular for vehicle applications when compared to dc and other ac motors. Another aspect in induction motor drives which has been researched recently is the use of multiphase induction motors where

the number of stator phases is more than three.

Here, a multi-phase system is a system with more than three stator phases. Among the different multi-phase induction motor drives being researched, the dual-3-phase solution can generate higher torque as compared to conventional three phase motor. This characteristic makes them convenient in high power and/or high current applications, such as ship propulsion, aerospace applications, and electric / hybrid vehicles. Output Torque of multiphase induction motors is much higher than that of conventional three phase Induction Motor, turning it in a much more interesting and suitable option for our purpose.

## Motivation and the substantiation of six phase squirrel cage motor:

Multiphase motor drives have been proposed for different applications where some specific advantages like: higher provided torque, lower torque pulsations, less spatial harmonics, less noise, higher overall system reliability, better power distribution per phase... can be better exploited, justifying the higher complexity in contrast to the three-phase solution. Some of the most suitable applications are the high current ones, like in electrical vehicles.

Since the power switches rated current is reduced proportionally with the number of phases, an increment in the number of power switches does not represent an additional cost. On the contrary, the cost is reduced by the "non-linearity" of the component prices. However, the system cost is penalized by the increased number of the current sensors, gate drive circuits, additional circuitry power supply, etc., while the system complexity is also increased by the new difficulties with the applied control techniques.

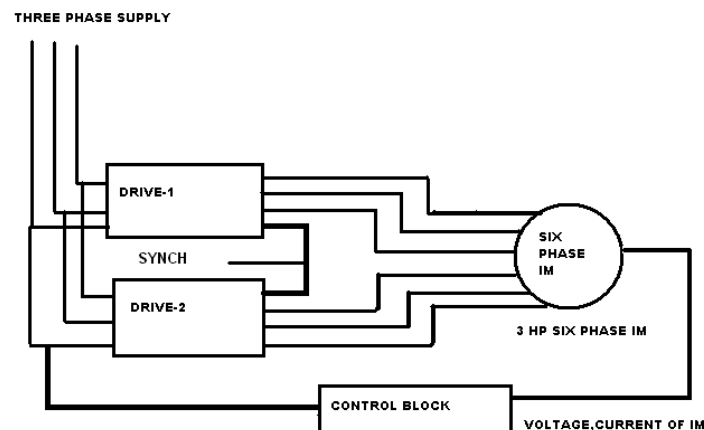


*Fig. 4dual-3-phase motor*

Among the different multi-phase induction drives solutions, the dual-3-phase induction machine having two stator winding sets spatially shifted by 60 electrical degrees has important advantages in applications like, where the low available DC-link voltage imposes high phase current.

The current stress of each semiconductor power device is reduced by one half compared with the 3-phase machine counterpart, while the dual-3-phase solution can benefit of the wide availability of components dedicated to 3-phase systems.

Moreover, Conventional 3-phase drives have been extensively used in industry applications, however, if one of the phases is lost, the rotatory field also disappears and the machine stops. The multi-phase drives offer the improvement of the system reliability, which is of great interest in specialized applications such as electric/hybrid vehicles. Independently of the number of phases the multi-phase machine has, it only needs two degrees of freedom to generate a rotatory field. Consequently, if one phase is lost the drive continues operating although at different rating values table X. Because of this reason, during the last three decades there is a growing interest to research several issues related to the use of multi-phase drives as a potential alternative for the conventional three-phase systems in electric vehicles.

In order to explore fault tolerance in terms of the loss of a phase, a number of idealizing assumptions may be made in relation to strategies on how the remaining un-faulted phases are controlled after the fault.

The following three cases are considered:

- Strategy 1: Keep the currents in the remaining un-faulted phases at their pre-fault values, in terms of both magnitude and phase. This reduces the stator joule loss by a factor  $(n-2)/n$ .
- Strategy 2: Increase the magnitude of the current in each un-faulted phase by a factor  $p$  ( $n/(n-2)$ ). This will maintain the stator joule loss at its pre-fault value.
- Strategy 3: Increase the magnitude of the current in each un-faulted phase by a factor  $n/(n-2)$ . This increases the stator joule loss by a factor  $n/(n-2)$ , but maintains the torque and rotor joule loss at their pre-fault value.

The data presented in Table 4 are based on a typical fan or propeller load, with the load torque which varies as the square of the speed, like it is happening with the resistance of air. In addition, it is assumed that the motor is operating on the steep part of its torque/speed characteristic so that the torque developed is proportional to slip. Furthermore, the data in Table 4 take no account of the additional rotor losses that arise because of the harmonic fields that will be present when the stator is no longer fully balanced.



**Table 4: Changes to output power and loss for multiphase machines with one phase open-circuited, assuming a speed-square-law load torque and a pre-fault slip of 0.01**

Phase number	Strategy	Post-fault slip	$\Delta P_{out}$ (%)	Change in stator loss (%)	Change in rotor loss (%)
6	1	0.01427	-1.29	-16.7	+42.7
	2	0.01195	-0.59	0.0	+19.5
	3	0.01000	0.00	+20.0	0.0
9	1	0.01259	-0.78	-11.1	+25.9
	2	0.01122	-0.37	0.0	+12.2
	3	0.01000	0.00	+12.5	0.0
12	1	0.01186	-0.56	-8.3	+18.6
	2	0.01089	-0.27	0.0	+8.9
	3	0.01000	0.00	+9.1	0.0
15	1	0.01145	-0.44	-6.7	+14.5
	2	0.01070	-0.21	0.0	+7.0
	3	0.01000	0.00	+7.1	0.0

*Fig. 5 Changes to output power with a fault on one phase*

Also, as a consequence of reductions of harmonics by increasing phases, the losses by Joule effect may experience a drop, but since the frequencies are bigger in the stator, they are more representative:

**Table 3: Reduction in stator joule loss achieved by increasing the number of phases beyond three**

Phase number, $n$	5	6	9	12	15	$\infty$
Stator copper loss reduction (%)	5.6	6.7	7.9	8.3	8.5	8.8

*Fig. 6 Reduction of stator losses*

All the benefits mentioned before give us the necessary push for making and investment in time and resources in implementing dual-3-phase system in electric vehicles.

## Overview of the literature:

Since an induction motor with dual-3-phase system has been chosen as the best solution for fulfill our requirements, a general vision of the fundamentals and principles of operating methods of this machines would be presented next.

### *Principal components*

A 3-phase induction motor (Fig.7) has two main parts: stationary stator and a revolving rotor. The rotor is separated from the stator by a small air gap that ranges from 0.4 mm to 4 mm, depending on the power of the motor.

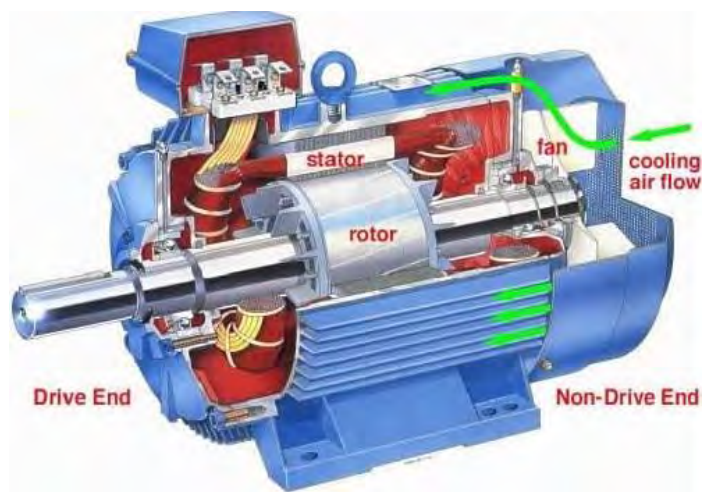
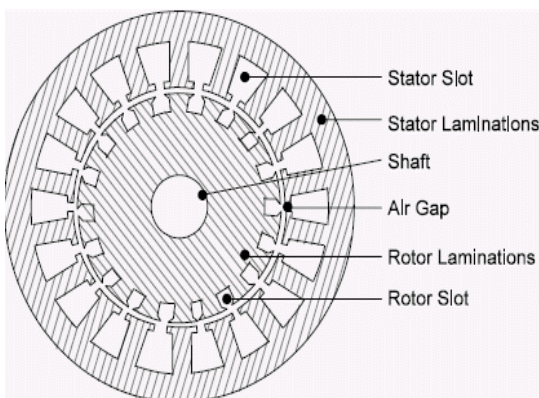


*Fig. 7 Three-phase induction motor.*

The stator (7) consists of a steel frame that supports a hollow, cylindrical core made up of stacked laminations. A number of evenly spaced slots, punched out of the internal circumference of the laminations, provide the space for the stator winding.



The rotor is also composed of punched laminations. These are carefully stacked to create a series of rotor slots to provide space for rotor winding. We use two types of rotor windings: (1) conventional 3-phase windings made of insulated wire and (2) squirrel-cage windings. The type of winding gives rise to two main classes of motors: squirrel cage induction motors (also called cage motors) and wound-rotor induction motors.

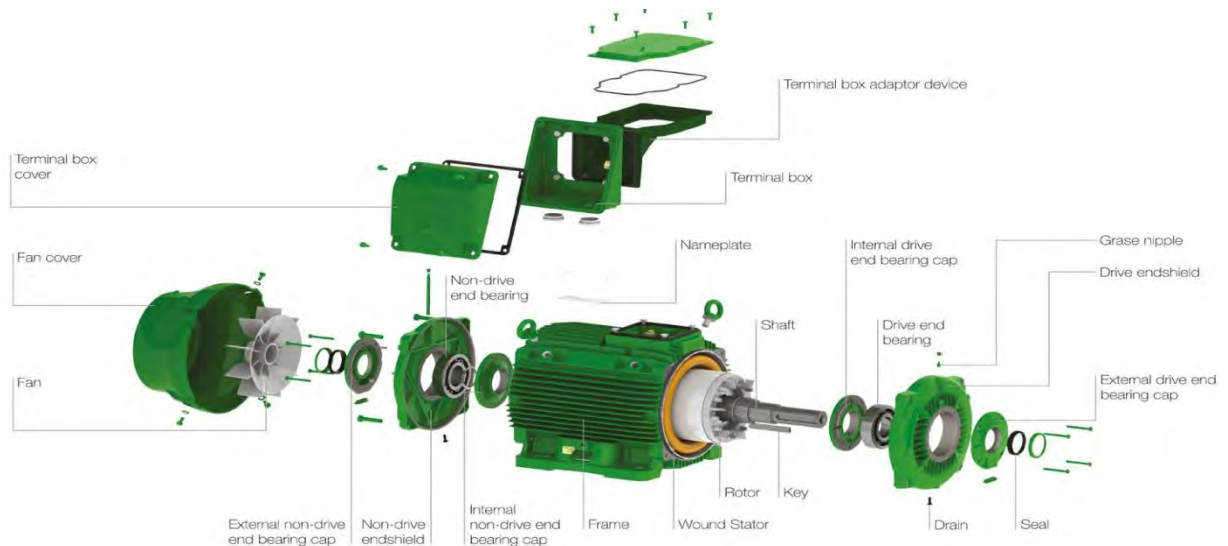
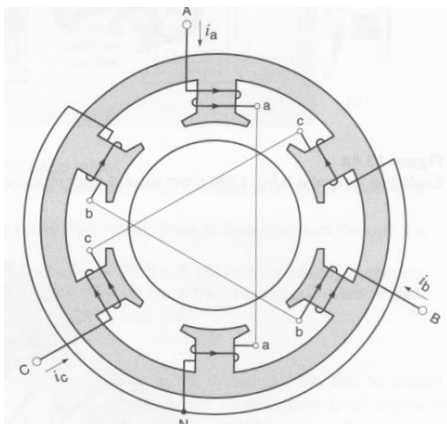


Fig. 8 Exploded view of the cage motor of Fig.7

Stator, rotor, end-bells, cooling fan, ball bearings, and terminal box. The fan blows air over the stator frame, which is ribbed to improve heat transfer. A squirrel-cage rotor is composed of bare copper bars, slightly longer than the rotor, which are pushed into the slots. The opposite ends are welded to two copper end-rings, so that all the bars are short-circuited together. The entire construction (bars and end-rings) resembles a squirrel cage, from which the name is derived. In small and medium-size motors, the bars and end-rings are made of die cast aluminum, molded to form an integral block.

A wound rotor has a 3-phase winding, similar to the one on the stator. The winding is uniformly distributed in the slots and is usually connected in 3 wire wyes. The terminals are connected to three slip rings, which turn with the rotor. The revolving slip-rings and associated stationary brushes enable us to connect external resistors in series with the rotor winding. The external resistors are mainly used during the start up period; under normal running conditions, the three brushes are short-circuited.

### Principle of operation: The Rotating Field and Induced Voltages



The operation of a n-phase induction motor is based upon the application of Faraday Law and the Lorentz force on a conductor.

Let's take as an example a three phase balanced system, consider a simple stator having 6 salient poles, each of which carries a coil having 5 turns(Fig.8). Coils that are diametrically opposite are connected in series by means of three jumpers that respectively connect terminals a-a, b-b, and c-c. This creates three identical sets of windings AN, BN, CN, that are mechanically spaced at 120

degrees to each other. The two coils in each winding produce magnetomotive forces that act in the same direction.

*Fig.8 Elementary stator having terminals A, B, C connected to a 3-phase source (not shown).*

The three sets of windings are connected in wye, thus forming a common neutral N. Owing to the perfectly symmetrical arrangement, the line to neutral impedances are identical. In other words, as regards terminals A, B, C, the windings constitute a balanced 3-phase system.

The result is illustrated in Fig.9. The rotating field will induce voltages in the phase coils AA, BB, and CC. Expressions for the induced voltages can be obtained by using Faraday laws of induction.

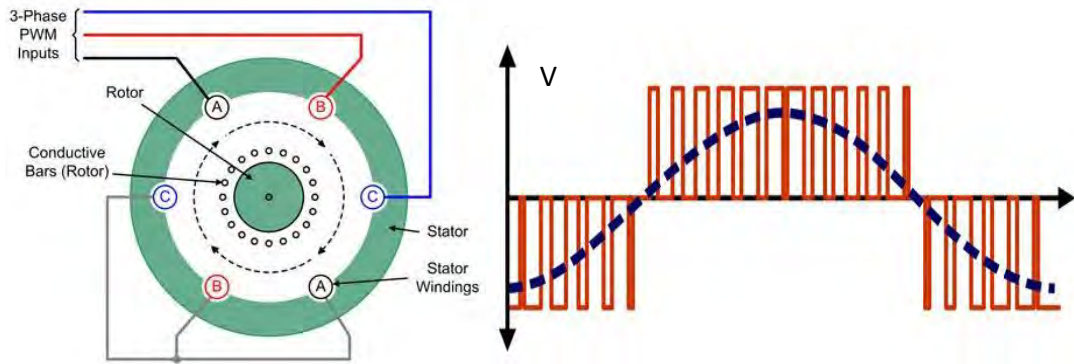


*Fig. 9 Air gap flux density distribution and signal from PWM.*

The flux density distribution in the air gap can be expressed as:

$$B(\theta) = B_{\max} \cos \theta \quad (1)$$

The air gap flux per pole,  $\phi_p$ , is:

$$\phi_p = \int_{-\pi/2}^{\pi/2} B(\theta) l r d\theta = 2B_{\max} l r \quad (2)$$

Where,

$l$  is the axial length of the stator.

$r$  is the radius of the stator at the air gap.

Let us consider that the phase coils are full-pitch coils of  $N$  turns (the coil sides of each phase are 180 electrical degrees apart as shown in Fig.9). It is obvious that as the rotating field moves (or the magnetic poles rotate) the flux linkage of a coil will vary.

The flux linkage for coil  $aa'$  will be maximum  $N\phi_p$  at  $\omega t = 0$  (Fig.9a) and zero at  $\omega t = 90$ . The flux

linkage  $\lambda_a(\omega t)$  will vary as the cosine of the angle  $\omega t$ . Hence;

$$\lambda_a(\omega t) = N\phi_p \cos \omega t \quad (3)$$

Therefore, the voltage induced in phase coil  $aa'$  is obtained from Faraday law as:

$$e_a = -\frac{d\lambda_a(\omega t)}{dt} = \omega N\phi_p \sin \omega t = E_{\max} \sin \omega t \quad (4)$$

The voltages induced in the other phase coils are also sinusoidal, but phase-shifted from each other by 120 electrical degrees. Thus,

$$e_b = E_{\max} \sin(\omega t - 120) \quad (5)$$

$$e_c = E_{\max} \sin(\omega t + 120) \quad (6)$$

\*360/n for n phases

From Equation (4), the rms value of the induced voltage is:

$$E_{rms} = \frac{\omega N\phi_p}{\sqrt{2}} = \frac{2\pi f}{\sqrt{2}} N\phi_p = 4.44 fN\phi_p \quad (7)$$

Where f is the frequency in hertz. Equation (7) has the same form as that for the induced voltage in transformers. However, P φ in Equation (7) represents the flux per pole of the machine.

Equation (7) shows the rms voltage per phase. The N is the total number of series turns per phase with the turns forming a concentrated full-pitch winding. In an actual AC machine each phase winding is distributed in a number of slots for better use of the iron and copper and to improve the wave form as we will see after in the real design of our motor. For such a distributed winding, the EMF induced in various coils placed in different slots are not in time phase, and therefore the phasor sum of the EMF is less than their numerical sum when they are connected in series for the phase winding. A reduction factor KW, called the winding factor, must therefore be applied. For most three-phase machine windings KW is about 0.85 to 0.95.

Therefore, for a distributed phase winding, the rms voltage per phase is  $E_{rms} = 4.44 fN\phi_p \text{ pKW}$  (8)

Where Nφ is the number of turns in series per phase.

## Running Operation

If the stator windings are connected to a three-phase supply and the rotor circuit is closed, the induced voltages in the rotor windings produce rotor currents that interact with the air gap field to produce torque. The rotor, if free to do so, will then start rotating. According to Lenz law, the rotor rotates in the direction of the rotating field such that the relative speed between the rotating field and the rotor winding decreases. The rotor will eventually reach a steady-state speed n that is less than the synchronous speeds at which the stator rotating field rotates in the air gap. It is obvious that at  $n = n_s$  there will be no induced voltage and current in the rotor circuit and hence no torque.

In a P-pole machine, one cycle of variation of the current will make the mmf wave rotate by  $2/P$  revolutions. The revolutions per minute  $n$  (rpm) of the traveling wave in a P-pole machine for a frequency  $f$  cycles per second for the currents are:

$$n = \frac{2}{P} f * 60 = \frac{120f}{p} \quad (9)$$

The difference between the rotor speed  $n$  and the synchronous speed  $n_s$  of the rotating field is called the slip  $s$  and is defined as

$$s = \frac{n_s - n}{n_s} \quad (10)$$

If you were sitting on the rotor, you would find that the rotor was slipping behind the rotating field by the slip rpm =  $n_s - n = sn_s$ . The frequency  $f_2$  of the induced voltage and current in the rotor circuit will correspond to this slip rpm, because this is the relative speed between the rotating field and the rotor winding. Thus, from Equation (9):

$$f_2 = \frac{P}{120} (n_s - n) = \frac{P}{120} sn_s = sf_1 \quad (11)$$

This rotor circuit frequency  $f_2$  is also called slip frequency. The voltage induced in the rotor circuit at slip  $s$  is:  $E_2s = 4.44 f_2 N_2 \phi p KW_2 = 4.44 sf_1 N_2 \phi p KW_2 = sE_2$  (12)

Where  $E_2$  is the induced voltage in the rotor circuit at standstill, that is, at the stator frequency  $f_1$ . The induced currents in the three-phase rotor windings also produce a rotating field. Its speed (rpm)  $n_2$  with respect to rotor is:

$$n_2 = \frac{120f_2}{p} = \frac{120sf_1}{p} = sn_s \quad (13)$$

Because the rotor itself is rotating at  $n$  rpm, the induced rotor field rotates in the air gap at speed  $n + n_2 = (1 - s)n_s + sn_s = ns$  rpm. Therefore, both the stator field and the induced rotor field rotate in the air gap at the same synchronous speed  $n_s$ . The stator magnetic field and the rotor magnetic field are therefore stationary with respect to each other. The interaction between these two fields can be considered to produce the torque. As the magnetic fields tend to align, the stator magnetic field can be visualized as dragging the rotor magnetic field.

### *Equivalent Circuit of the Induction Motor*

Finally, we develop the equivalent circuit of an asynchronous generator and determine its properties under load.

A 3-phase wound-rotor induction motor is very similar in construction to a 3-phase transformer. Thus, the motor has 3 identical primary windings and 3 identical secondary windings one set for each phase. On account of the perfect symmetry, we can consider a single primary winding and a single secondary winding in analyzing the behavior of the motor.

When the motor is at standstill, it acts exactly like a conventional transformer, and so its equivalent circuit (Fig.10) is the same as that of a transformer, previously developed.

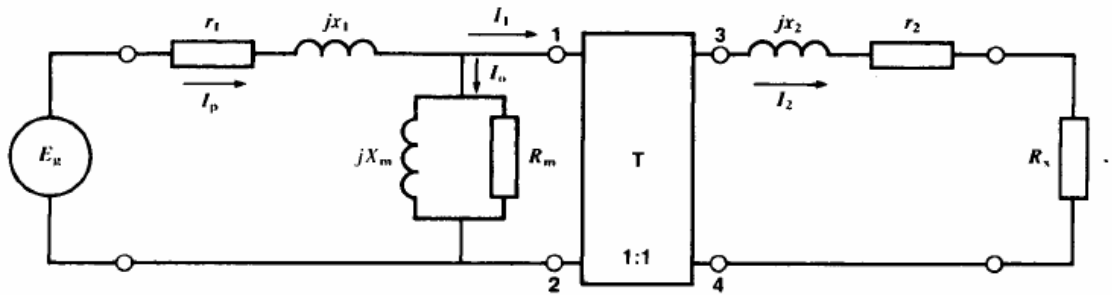


*Fig. 10 Equivalent circuit of a wound-rotor induction motor at standstill.*

In the case of a conventional 3-phase transformer, we would be justified in removing the magnetizing branch composed of  $jX_m$  and  $R_m$  because the exciting current  $I_o$  is negligible compared to the load current  $I_P$ . However, in a motor this is no longer true:  $I_o$  may be as high as 40 % of  $I_P$  because of their gap. Consequently, we cannot eliminate the magnetizing branch. The stator and rotor winding can be

represented as shown in Fig.11 (a) and (b),

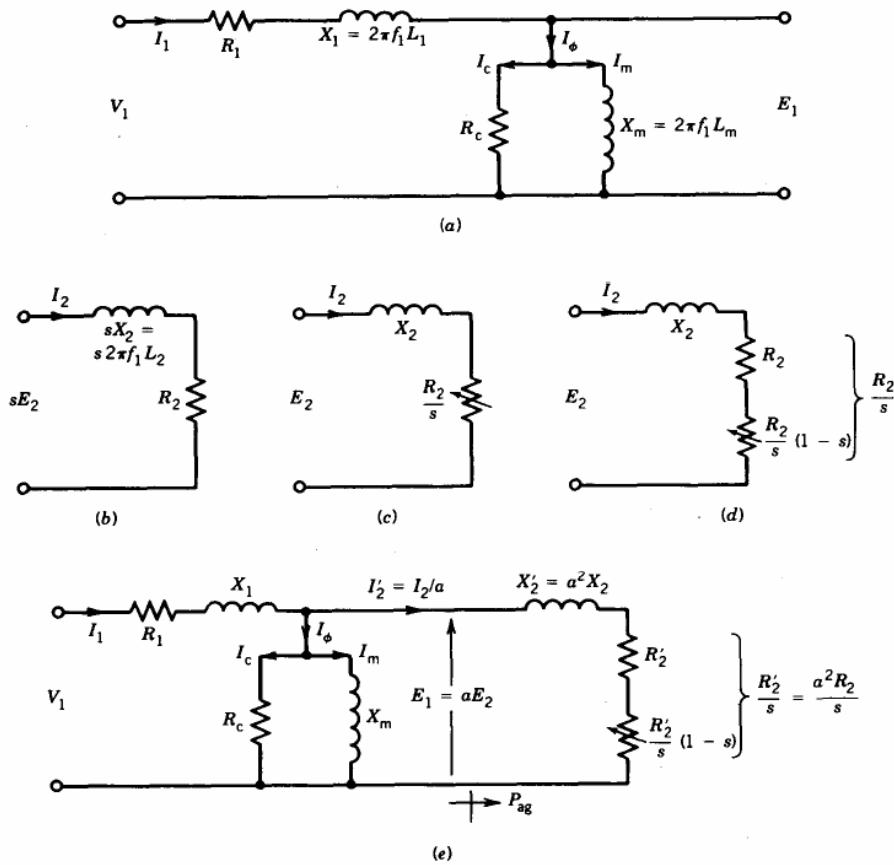


Fig. 11 Development of the induction machine equivalent circuit

where,

$V_1$  = per-phase terminal voltage.

$R_1$  = per-phase stator winding resistance.

$L_1$  = per-phase stator leakage inductance.

$E_1$  = per-phase induced voltage in the stator winding

$L_m$  = per-phase stator magnetizing inductance

$R_c$  = per-phase stator core loss resistance.

$E_2$  = Per-phase induced voltage in rotor at standstill (i.e., at stator frequency  $f$ .)

$R_2$  = Per-phase rotor circuit resistance

$L_2$  = Per-phase rotor leakage inductance

Note that there is no difference in form between this equivalent circuit and that of the transformer primary winding. The difference lies only in the magnitude of the parameters. For example, the excitation current  $I_0$  is considerably larger in the induction machine because of the air gap. In induction machines it is as high as: 30 to 50 percent of the rated current, depending on the motorize, whereas it is only 1 to 5 percent in transformers. Moreover, the leakage reactance  $X_1$  is larger because of the air gap and also



because the stator and rotor windings are distributed along the periphery of the air gap rather than concentrated on a core, as in the transformer.

Note that the rotor circuit frequency and current are:  $f_2$  and  $I_2$ .

$$I_2 = \frac{sE_2}{R_2 + jsX_2} \quad (14)$$

The power involved in the rotor circuit is:

$$P_2 = I_2^2 R_2 \quad (15)$$

Which represents the rotor copper loss per phase. Equation (14) can be rewritten as:

$$I_2 = \frac{E_2}{(R_2/s) + jX_2} \quad (16)$$

Equation (16) suggests the rotor equivalent circuit of Fig.11b. Although the magnitude and phase angle of  $I_2$  are the same in Equations (14) and (16), there is a significant difference between these two equations and the circuits (Figs.11b and 11c) they represent. The current  $I_2$  in Equation (14) is at slip frequency  $f_2$ , whereas  $I_2$  in Equation (16) is at line frequency  $f_1$ . In Equation (14) the rotor leakage reactance  $sX_2$  varies with speed but resistance  $R_2$  remains fixed, whereas in Equation (16) the resistance  $R_2/s$  varies with speed but the leakage reactance  $X_2$  remains unaltered. The per phase power associated with the equivalent circuit of Fig.11c is:

$$P = I_2^2 \frac{R_2}{s} = \frac{P_2}{s} \quad (17)$$

Because induction machines are operated at low slips (typical values of slip  $s$  are 0.01 to 0.05) the power associated with Fig.11c is considerably larger. Note that the equivalent circuit of Fig.11c is at the stator frequency, and therefore this is the rotor equivalent circuit as seen from the stator. The power in Equation (17) therefore represents the power that crosses the air gap and thus includes the rotor copper loss as well as the mechanical power developed. Equation (17) can be rewritten as:

$$P = P_{ag} = I_2^2 \left[ R_2 + \frac{R_2}{s}(1-s) \right] = I_2^2 \frac{R_2}{s} \quad (18)$$

The corresponding equivalent circuit is shown in Fig.11d. The speed dependent resistance  $R_2 (1-s)/s$  represents the mechanical power developed by the induction machine.

$$P_{mech} = I_2^2 \frac{R_2}{s} (1-s) \quad (19)$$

$$P_{mech} = (1-s) * P_{ag} \quad (20)$$

$$P_{mech} = \frac{(1-s)}{s} P_2 \quad (21)$$

$$P_2 = I_2^2 R_2 = s P_{ag} \quad (22)$$

and,

$$P_{ag} : P_2 : P_{mech} = 1 : s : (1-s) \quad (23)$$

Thus,

Equation (23) indicates that, of the total power input to the rotor (i.e., power crossing the air gap,  $P_{ag}$ ), a fraction  $s$  is dissipated in the resistance of the rotor circuit (known as rotor copper loss) and the fraction  $1-s$  is converted into mechanical power. Therefore, for efficient operation of the induction machine, it should operate at a low slip so that more of the air gap power is converted into mechanical power. Part of the mechanical power will be lost to overcome the windage and friction. The remainder of the mechanical power will be available as output shaft power.

\*Since we are modeling the motor, and we don't have the physical prototype, the methods for real measuring determination of these parameters (locked rotor and no-load test) are not going to be included.

### Performance Characteristics

The equivalent circuits derived in the preceding section can be used to predict the performance characteristics of the induction machine. The important performance characteristics in the steady state are the efficiency, power factor, current, starting torque, maximum (or pull-out) torque, and so forth as we will see.

The mechanical torque developed  $T_{mech}$  per phase is given by

$$P_{mech} = T_{mech} \omega_{mech} = I_2^2 \frac{R_2}{s} (1-s) \quad (45)$$

$$\omega_{mech} = \frac{2\pi n}{60} \quad (46)$$

Where

The mechanical speed mech  $\omega$  is related to the synchronous speed:  $\omega_{mech} = (1-s)\omega_{syn}$  (4.47)

$$\omega_{mech} = \frac{n_{syn}}{60} 2\pi(1-s) \quad (48)$$

and

$$\omega_{syn} = \frac{120f}{60P} * 2\pi = \frac{4\pi f_1}{P} \quad (49)$$

From Equations (45), (47), and (18)

$$T_{mech} \omega_{syn} = I_2^2 \frac{R_2}{s} = P_{ag} \quad (50)$$

$$T_{mech} = \frac{1}{\omega_{syn}} P_{ag} \quad (51)$$

Then,

$$T_{mech} = \frac{1}{\omega_{syn}} I_2^2 \frac{R_2}{s} \quad (52)$$

$$T_{mech} = \frac{1}{\omega_{syn}} I_2'^2 \frac{R_2'}{s} \quad (53)$$

From the equivalent circuit and Equation (53)

$$T_{mech} = \frac{1}{\omega_{syn}} * \frac{V_{th}^2}{(R_{th} + R_2'/s)^2 + (X_{th} + X_2')^2} * \frac{R_2'}{s} \quad (54)$$

Note that if the approximate equivalent circuits are used to determine  $I_2$ , in Equation (54),  $V_{th}$ ,  $R_{th}$ , and  $X_{th}$  should be replaced by  $V_1$ ,  $R_1$ , and  $X_1$ , respectively. The prediction of performance based on the approximate equivalent circuit may differ by 5 percent from those based on the equivalent circuit.

For a m-phase machine (as in our case), Equation (54) should be multiplied by m to obtain the total torque developed by the machine. The torque-speed characteristic is shown in Fig.14. At low values of slip,

$$R_{th} + \frac{R'_2}{s} \gg X_{th} + X'_2 \text{ and } \frac{R'_2}{s} \gg R_{th} \quad (55)$$

Thus

$$\text{Thus } T_{mech} \cong \frac{1}{\omega_{syn}} * \frac{V_{th}^2}{R'_2} * s \quad (56)$$

The linear torque-speed relationship is evident in Fig.4.14 near the synchrony speed. Note that if the approximate equivalent circuits are used, in Equation (56)  $V_{th}$  should be replaced by  $V_1$ . At larger values of slip,

$$R_{th} + \frac{R'_2}{s} \ll X_{th} + X'_2 \quad (57)$$

And

$$T_{mech} = \frac{1}{\omega_{syn}} * \frac{V_{th}^2}{(X_{th} + X'_2)^2} * \frac{R'_2}{s} \quad (58)$$

The torque varies almost inversely with slip near  $s = 1$ , as seen from Fig.12.

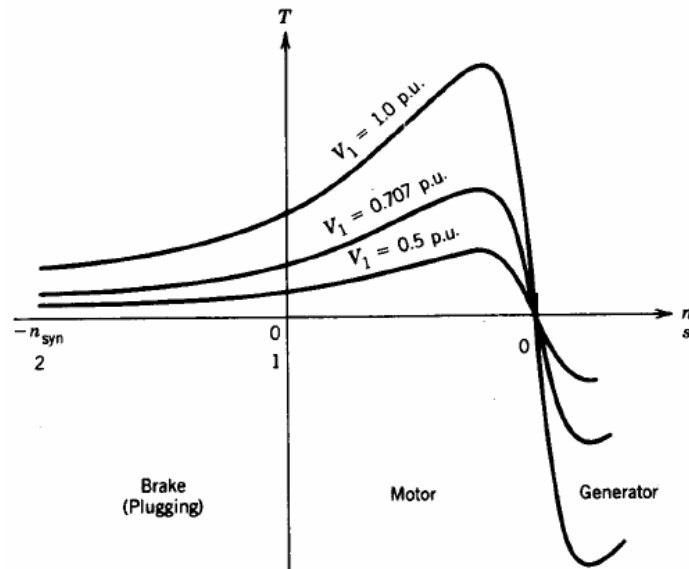


*Fig. 12 Torque-speed profile at different voltages.*

Equation (49) also indicates that at a particular speed (i.e., a fixed value of  $s$ ) the torque varies as the square of the supply voltage  $V_{th}$  (hence  $V_1$  Fig.12) shows the  $T$ - $n$  profile at various supply voltages.

An expression for maximum torque can be obtained by setting  $dT / ds = 0$ . Differentiating Equation (54) with respect to slip  $s$  and equating the results to zero gives the following condition for maximum torque:

$$\frac{R'_2}{S_{T_{\max}}} = \sqrt{R_{th}^2 + (X_{th} + X'_2)^2} \quad (59)$$

This expression can also be derived from the fact that the condition for maximum torque corresponds to the condition for maximum air gap power (Equation (51)). This occurs, by the familiar impedance-matching principle in circuit theory, when the impedance of  $sR / 2'$  equals in magnitude the impedance between it and the supply voltage  $V_1$  as shown in Equation (59). The slip  $S_{T_{\max}}$  at maximum torque  $T_{\max}$  is:

$$S_{T_{\max}} = \frac{R'_2}{\sqrt{R_{th}^2 + (X_{th} + X'_2)^2}} \quad (60)$$

The maximum torque per phase from Equations (49) and(60) is:

$$T_{\max} = \frac{1}{2\omega_{syn}} * \frac{V_{th}^2}{R_{th} + \sqrt{R_{th}^2 + (X_{th} + X'_2)^2}} \quad (61)$$

Equation (61) shows that the maximum torque developed by the induction machine is independent of the rotor circuit resistance. However, from Equation (60) it is evident that the value of the rotor circuit resistance  $R_2$  determines the speed at which this maximum torque will occur. The torque speed characteristics for various values of  $R_2$  are shown in Fig.13. In a wound rotor induction motor, external resistance is added to the rotor circuit to make the maximum torque occur at standstill so that high starting torque can be obtained. As the motor speeds up, the external resistance is gradually decreased and finally taken out completely. Some induction motors are, in fact, designed so that maximum torque is available at start, that is, at zero speed.

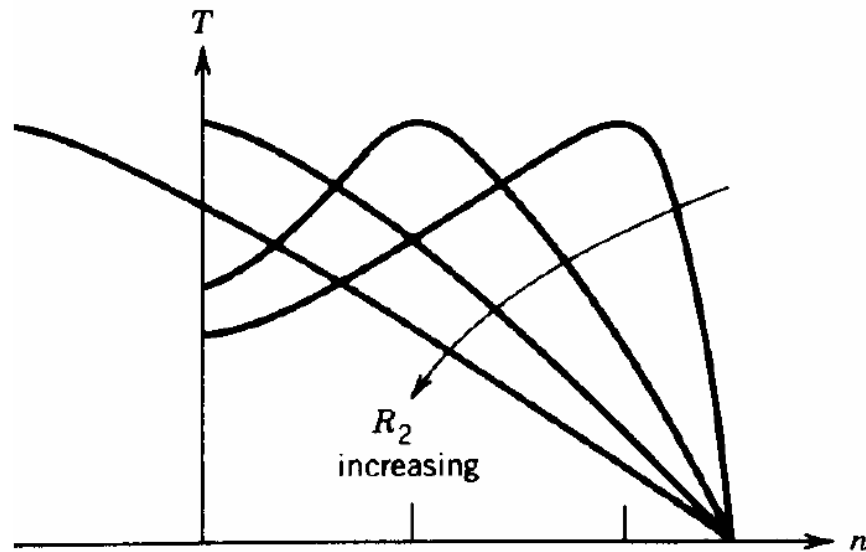


*Fig. 13 Torque speed characteristics for varying  $R_2$ .*

If the stator resistance  $R_1$  is small (hence  $R_{th}$  is negligibly small), from Equations (60) and (61),

$$s_{T_{\max}} \cong \frac{R'_2}{X_{th} + X'_2} \quad (62)$$

$$T_{\max} = \frac{1}{2\omega_{syn}} * \frac{V_{th}^2}{X_{th} + X'_2} \quad (63)$$

Equation (63) indicates that the maximum torque developed by an induction machine is inversely proportional to the sum of the leakage reactances.

From Equation (54), the ratio of the maximum developed torque to the torque developed at any speed is:

$$\frac{T_{\max}}{T} = \frac{(R_{th} + R'_2 / s)^2 + (X_{th} + X'_2)^2}{(R_{th} + R'_2 / s_{T_{\max}})^2 + (X_{th} + X'_2)^2} * \frac{s}{s_{T_{\max}}} \quad (64)$$

If R1 (hence Rth ) is negligibly small,

$$\frac{T_{\max}}{T} = \frac{(R'_2 / s)^2 + (X_{th} + X'_2)^2}{(R'_2 / s_{T_{\max}})^2 + (X_{th} + X'_2)^2} * \frac{s}{s_{T_{\max}}} \quad (65)$$

From Equations (62) and (65)

$$\frac{T_{\max}}{T} = \frac{(R'_2 / s)^2 + (R'_2 / s_{T_{\max}})^2}{2(R'_2 / s_{T_{\max}})^2} * \frac{s}{s_{T_{\max}}} \quad (66)$$

$$\frac{T_{\max}}{T} = \frac{s_{T_{\max}}^2 + s^2}{2 * s_{T_{\max}} * s} \quad (67)$$

Equation (67) shows the relationship between torque at any speed and the maximum torque in terms of their slip values.

## Efficiency

In order to determine the efficiency of the induction machine as a power converter, the various losses in the machine are first identified. These losses are illustrated in the power flow diagram of Fig.4.16. For a 3  $\phi$  machine the power input to the stator is:

$$P_{in} = 3V_1 I_1 \cos \theta_1 \quad (68)$$

The power loss in the stator winding is:

$$P_1 = 3I_1^2 R_1 \quad (69)$$

Where R1 is the AC resistance (including skin effect) of each phase winding at the operating temperature and frequency.

Power is also lost as hysteresis and eddy current loss in the magnetic material of the stator core.

The remaining power,  $P_{ag}$ , crosses the air gap. Part of it is lost in the resistance of the rotor circuit. Where  $R_2$  is the ac resistance of the rotor winding. If it is a wound-rotor machine,  $R_2$  also includes any external resistance connected to the rotor circuit through slip rings. Power is also lost in the rotor core. Because the core losses are dependent on the frequency  $f_2$  of the rotor, these may be negligible at normal operating speeds, where  $f_2$  is very low.

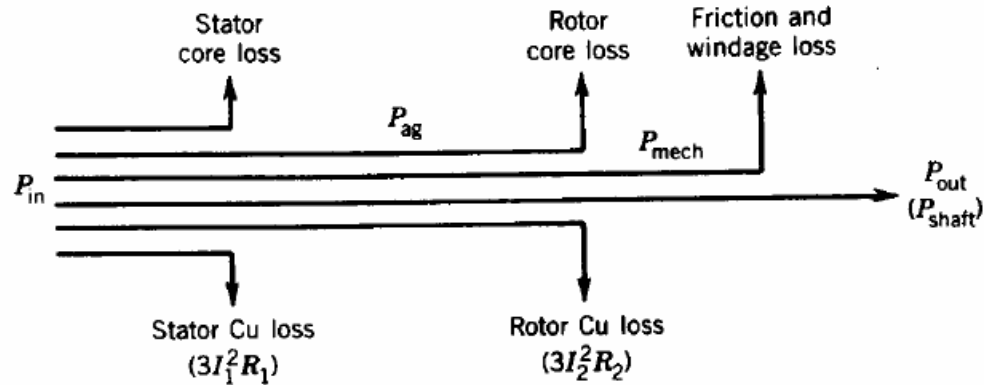


Fig. 14 Power flow in an induction motor.

The remaining power is converted into mechanical form. Part of this is lost as wind age and friction losses, which are dependent on speed. The rest is the mechanical output power  $P_{out}$ , which is the useful power output from the machine.

The efficiency of the induction motor is:

$$\eta = \frac{P_{out}}{P_{in}} \tag{71}$$

The efficiency is highly dependent on slip. If all losses are neglected except those in the resistance of the rotor circuit,

$$P_{ag} = P_{in} \tag{72}$$

$$P = sP_{ag} \tag{73}$$

$$P_{out} = P_{mecj} = P_{ag}(1 - s) \tag{74}$$

And the ideal efficiency is: (  $s$  )

$$\eta_{ideal} = \frac{P_{out}}{P_{in}} = (1 - s) \tag{75}$$



Sometimes ideal  $\eta$  is also called the internal efficiency as it represents the ratio of the power output to the air gap power. It indicates that an induction machine must operate near its synchronous speed if high efficiency is desired. This is why the slip is very low for normal operation of the induction machine.

If other losses are included, the actual efficiency is lower than the ideal efficiency of Equation (75). The full-load efficiency of a large induction motor may be as high as 95 percent.

\* Other operation modes (generating and braking) are not going to be included since is not the purpose of the research.

### Motor Design Classes

Since different applications need different characteristics from induction motors, it has been specified different classes of induction motor, with different characteristics. Typical torque speed-curves for classes A-D are sketched below.

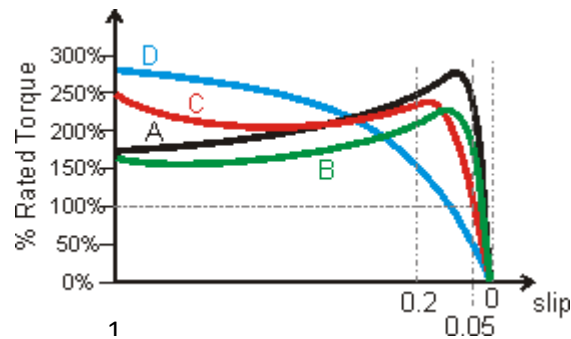


Fig. 15 motor classes

Motor Classes A and D are obtained by designing the rotor resistance to be either low (class A) or high (class D). Classes B and C are obtained by exploiting the effect of skin depth to obtain a variable resistance rotor circuit. Squirrel-cage motors are intentionally designed to develop a higher starting torque by utilizing the skin effect in the rotor bars. This, in turn, affects the stator currents as well.

To analyze the characteristics of these machines in non-steady-state operations with higher rotor slip, e.g., start with SCR based AC voltage controller or simple Y-D starter, the skin effect in rotor bars (also known as deep ) has to be taken into consideration.

order to obtain valid results for torque and stator currents during ramp-up. Example rotor conductor designs for classes A through D are shown below. Comparing classes A and B, class B has a deeper bar to exploit skin depth effects. The bar width may vary in order to enhance this effect. Class C rotors are typically fabricated with two separate cages. Only the outer cage will conduct at starting. There is air between the cages and at the top of the slot (to reduce leakage flux). Note that cast rotor designs must have a closed slot design to prevent molten aluminum from escaping. Class D has a small conductor, giving a high resistance at all slips. The class D example shown has an open slot, for a fabricated rotor design.

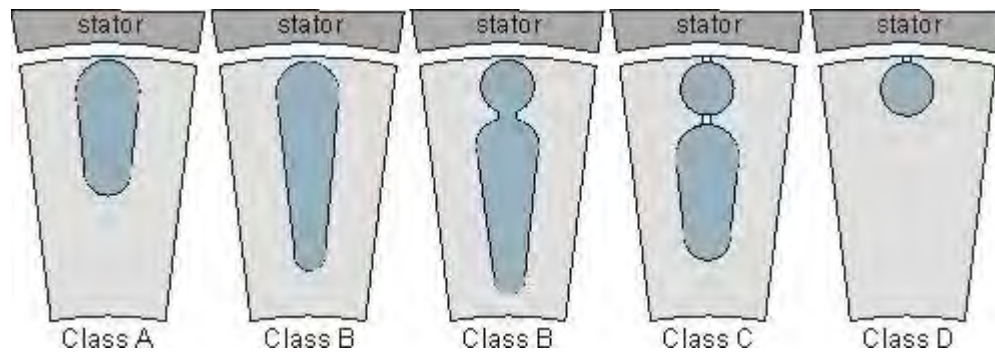


Fig. 16 slot shapes

A summary of the performance of the motor classes is provided in the table below

	<b>Class A</b>	<b>Class B</b>	<b>Class C</b>	<b>Class D</b>
Type	General Purpose	General Purpose	High Starting Torque	Very High Starting Torque
Start Torque	100% rated for larger motors, 200% rated, smaller motors	100% rated for larger motors, 200% rated, smaller motors	Approx 250% rated	> 275% rated
Start Current	~800% rated	500%-600% rated		
Pullout Torque	200%-300% rated	≥200% rated	Slightly lower than class A	
Pullout Slip	<0.2	<0.2		High, can be as much as 1.0
Rated Slip	<0.05, lower than similar sized class B	must be <0.05, usually <0.03	<0.05, higher than class B	High, typically 0.07 to 0.11, can be up to 0.17
Applications	Fans, Blowers, Pumps, Machine Tools	As for Class A	Compressors, pumps, conveyors	High inertia applications, e.g. mechanical punches
Notes	High starting inrush current causes power system problems, it can cause the supply voltage to sag and requires special starting techniques. More efficient than same sized class B	Replacements for Class A due to lower start current. The standard off-the shelf commodity motor.	Applications that require high start torques. Note that the pull-up and pull-out torque can both be lower than the start torque. Less efficient than class B	Very high inertia applications. e.g. in a punch or reciprocal pump where the slip may vary between 0 and 0.50 Much less efficient than other designs

Fig. 17 class motor table

## *Design Trends & Influences*

### *Energy Efficient Design*

The techniques to make a more efficient motor are well understood:

1. Use thicker conductors. Increasing the cross-section of the conductors will result in lower  $I^2R$  losses.
2. Increase the length of the machine. A longer machine requires a lower torque density, which means a lower flux density. Lower flux density will result in lower iron losses.
3. Increase the outer diameter of the stator. Increased outer diameter means an increased surface area, allowing more effective cooling. This in turn means that a smaller, lower power fan can be used
4. Use a low loss lamination steel. Lamination steels can be bought in different grades, with variable hysteresis losses. Laminations can also be bought in various thicknesses, with thinner laminations resulting in lower eddy current losses. A thin low-loss lamination will have significantly lower iron loss than an thicker standard lamination
5. Ensure that the air gap length is constant. If the air gap surfaces are machined to give a constant air gap, there will be smaller variations in flux density and therefore reduced likelihood of concentrations of iron losses. (Eddy current losses are a function of flux density squared.)

### *Factors limiting the use of higher efficiency motors*

The first limit on uptake of premium efficiency motors is cost. Reviewing the above options to improve efficiency, 1-3 require more material to be put into the motor, increasing material costs. Option 4 requires more expensive laminations (thinner laminations and low loss steel are both more expensive). In addition, if thinner laminations are used, more laminations are required for a given length of machine, resulting in higher manufacturing costs (more lamination punches per machine, increased wear on punches, more difficult handling). Option 5 adds an additional step to the manufacturing process, again increasing manufacturing costs.

It can be seen that all the obvious options to improve motor efficiency result in more expensive machines. To maintain profitability, manufacturers must therefore increase the purchase price of a machine if it is more efficient.

From an end user point of view, the increased initial purchase price of a more efficient motor is more than offset by reduced lifetime operating costs. A premium efficiency motor will typically pay for itself in electricity savings in about 4 years (assuming constant operation). Typical motor lifetimes are around 20 years, so from a lifetime perspective, premium efficiency motors are a sound financial choice.

If premium efficiency motors are such a sound choice, the question must be asked why people don't buy premium efficiency motors. A number of reasons can be found:

- Most motor purchases are not made by the end user. They are made by "OEM"s: other equipment manufacturers. OEM's don't pay the operating costs of the motor and must keep their costs down to maintain their profitability.
- New equipment is purchased from capital budgets. This is typically independent of any future operating budget. Capital costs must usually be minimized during the development of a new facility and are typically funded by one-time fixed budgets. Once a facility is built, the operating costs are funded from another budget.
- Large users generate their own electricity. In a regulated electricity market, large users do not particularly care how much electricity they use, as long as it is lower than their generating capacity. With the advent of de-regulated markets and the possibility of selling excess generating capacity back to the grid, this is less of an issue.

A second limit on the development of premium efficiency motors has been standards. All motors in the small-medium (up to several hundred Hp) size range must be made to meet industrial standards. This limits the ability of manufacturers to be innovative with new motors. e.g. the maximum length and outside diameter are specified in the standard, so cannot be increased beyond a certain point to improve efficiency. In addition, standards specify minimum efficiency levels that must be met. Since all motors that meet the standard are viewed as equivalent, manufacturer A has no incentive to exceed the standard, as this would make its motors more expensive than those from manufacturer B who just meets the standard. In order to remain in business, the manufacturer must aim to meet the standards at minimum unit cost, which typically means *just* meeting the standard

## Standards

As we mentioned before in Objectives section, the IEC(International Electrotechnical Commission) is the organization that publishes consensus-based International Standards and manages conformity assessment systems for electric and electronic products, systems and services, collectively known as electrotechnology.

In this field we can focus in two main areas of interest, the efficiency and the construction.

In the efficiency IEC has developed an internationally applicable testing Standard IEC 60034-2-1 for electric motors and a classification scheme IEC 60034-30-1 with four levels of motor efficiency ("IE-code"):

Efficiency levels	Efficiency classes, IEC 60034-30 and Global 2008	Testing standard, IEC 60034-2-1, including stray-load losses, 2008	MEPS adopted in these countries
Standard	IE1	All	Brazil, China, Costa Rica, Israel, Taiwan
High efficiency	IE2		Australia, Canada, Mexico, New Zealand, United States, Korea (2008), Brazil (2009), China (2011), Europe (2012)
Premium efficiency	IE3		United States (2011)
Above-premium efficiency	IE4		

*Fig. 18 efficiency table*

The European Union sets motor MEPS( minimum energy performance standards) levels at IE3 (or IE2 in combination with a variable frequency drive) from 2015 for smaller motors and from 2017 covering also larger motors.

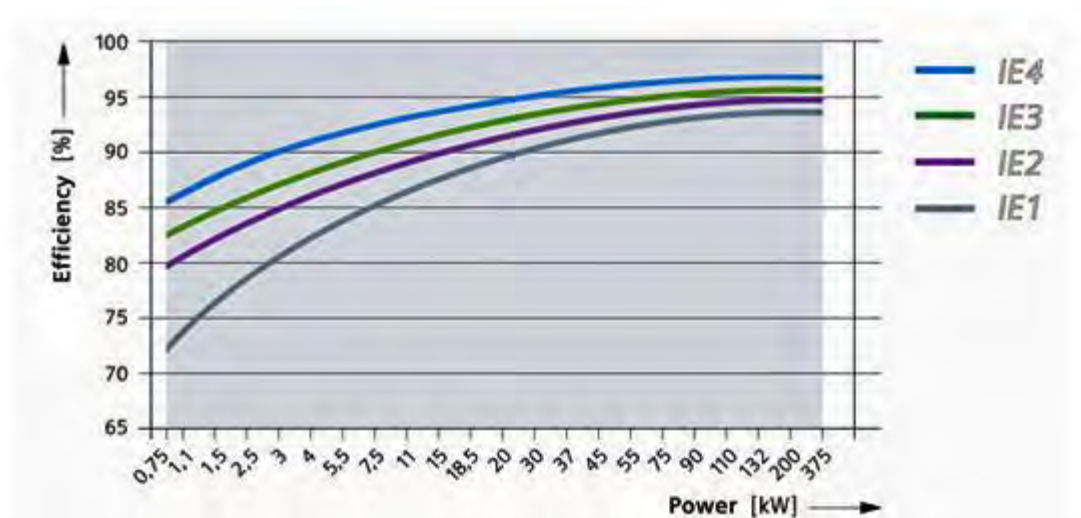


*Fig. 19 Efficiency graph*

In this table it is represented roughly the differences between the efficiency of IE levels in respect of the size of motor. This is just an approximation since the number of poles, frequency and the point of operation are not represented.

The other important area is the constructive characteristics of the motor. A motor is not composition of different parts and the IEC has a different committee and subcommittee for each the electrotechnical device or facility of study. The offered motor shall at the time of delivery comply with all the relevant standards and specifications, in particular the following:

Title	Standard
General requirements for rotating electrical machines	IEC 34-1 IEC 85
Fixing dimensions and assignment of rated output with IM B 3	IEC 72
Terminal markings and direction of rotation of rotating electrical machines	IEC 34-8
Types of construction of rotating electrical machines	IEC 34-7
Method of cooling rotating electrical machinery	IEC 34-6
Degrees of protection by enclosures for rotating electrical machinery	IEC 34-5
Vibration severity of electrical machines	IEC 34-14, ISO 2373
Parallel shaft extensions for electrical machines	IEC 72
Noise emission limits	IEC 34-9
Starting performance	IEC 34-12
IEC standard voltages	IEC 38
Methods for determining losses and efficiency of rotating electrical machinery from test	IEC 34-2

*Fig. 20 Motor standards specifications*

As it is understandable we are not including all the referent information because is not the purpose of the project, but we will show as example of major interest some of them because of it easy and quick understanding:

### *Types of duty*

Duty type	Designation	Duty type	Designation
S1	Continuous duty	S6	Continuous-operating periodic duty
S2	Short-time duty	S7	Continuous-operation periodic duty with electrical braking
S3	Intermittent periodic duty without starting	S8	Continuous-operation periodic duty with related load/speed changes
S4	Intermittent periodic duty with starting	S9	Duty with non-periodic and speed variations
S5	Intermittent periodic duty with electrical braking		

*Fig. 21 Types of duty*

Various types of duty have been defined in terms of how the load, and thus the output of the motor, varies with time. The rated output for each type of duty is determined in a load test which the motor must undergo without the temperature limits laid down in IEC Publication 34-1 (1994) being exceeded.

## Insulation

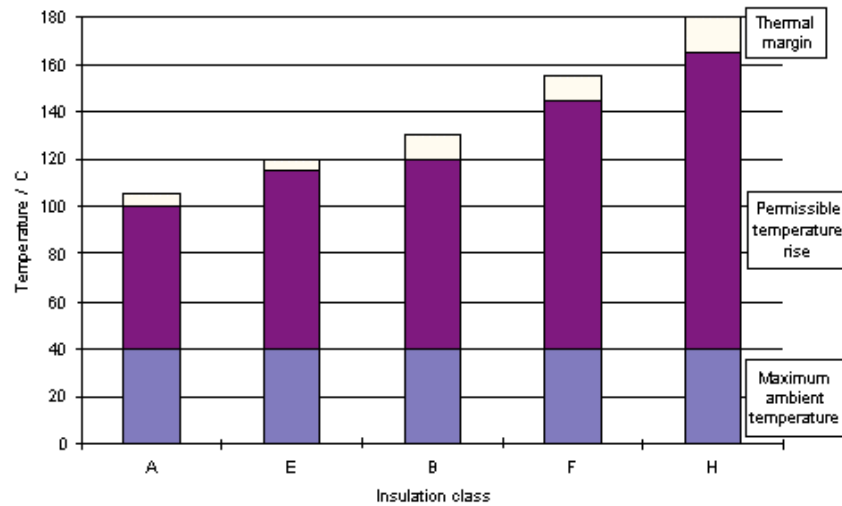


*Fig. 22 Types of insulation*

According to IEC 85, insulation is divided into insulation classes. Each class has a designation corresponding to the temperature that is upper limit of the range of applications of the insulation material under normal operating conditions and with satisfactory life. If this upper limit is exceeded, the life of the insulation will be shorten.

## Protection

Degree of protection are defined in IEC Publication 34-5 and are stated as the letters IP(International Protection) followed by two digits. The first digit states the degree of protection against contact and the penetration of solid objects.

First digit	Protection against contact and the entry of objects
0	No special protection of persons against accidental or inadvertent contact with live or moving parts. No protection of machine against ingress of solid foreign bodies
1	Protection against accidental or inadvertent contact with live and moving parts inside the enclosure by a large surface of human body. Protection against ingress of large solid foreign bodies (diameter greater than 50 mm).
2	Protection against contact by finger with live or moving parts inside the enclosure. Protection against ingress of small solid foreign bodies (diameter greater than 12 mm).
4	Protection against contact with live or moving parts inside the enclosure by tools, wires, or such objects of thickness greater than 1 mm. Protection against ingress of small solid foreign bodies (diameter > 1 mm) excluding the ventilation openings (intake and discharge of external fans) and the drain hole of enclosed machine which may have degree 2 protection.
5	Complete protection against contact with live or moving parts inside the enclosure. Protection against harmful deposits of dust. The ingress of dust is not totally prevented, but dust cannot enter in an amount sufficient to interfere with satisfactory operation of the machine.

*Fig. 23 Types of protection "a"*

The second digit states the degree of protection against water.

Second digit	Protection of harmful ingress of water
0	No special protection.
1	Dripping water (vertically falling drops) shall have no harmful effect.
2	Drop of water falling at any angle up to 15° from the vertical shall have no harmful effect.
3	Water falling as a spray at an angle equal to or smaller than 60° with respect to the vertical shall have no harmful effect.
4	Water splashed against the machine from any direction shall have no harmful effect.
5	Water protection by a nozzle against the machine from any direction shall have no harmful effect.
6	Water from heavy seas shall not enter the machine in harmful quantity.
7	Ingress of water into the machine in a harmful quantity shall not be possible when the machine is immersed in water under stated conditions of pressure and time.
8	Ingress of water into machine in a harmful quantity shall not be possible when the machine is immersed in water under a specified pressure and for an indefinite time.

*Fig. 24 Types of protection "b"*

A letter S added after the digits means that the machine has been tested when stationary. The letter W between IP and the digits indicates a weatherproof version; this means that the version is protected against harmful ingress of rain, snow and solid air-borne particles.

## Objectives

The aim of the project is to design the prototype of dual-3-phase motor that fulfill the necessities mentioned before in the introduction and meet all the standards imposed to this kind of motors. In the election of a six phases motor for our vehicle ,apart from the already mentioned advantages for electrical vehicles, the most critical reason has been the limitation of batteries voltage (80V).With the expression of mechanical torque provided by shaft by one single phase :

$$T_{mech} = \frac{1}{\omega_{syn}} * \frac{V_{th}^2}{(R_{th} + R_2' / s)^2 + (X_{th} + X_2')^2} * \frac{R_2'}{s}$$



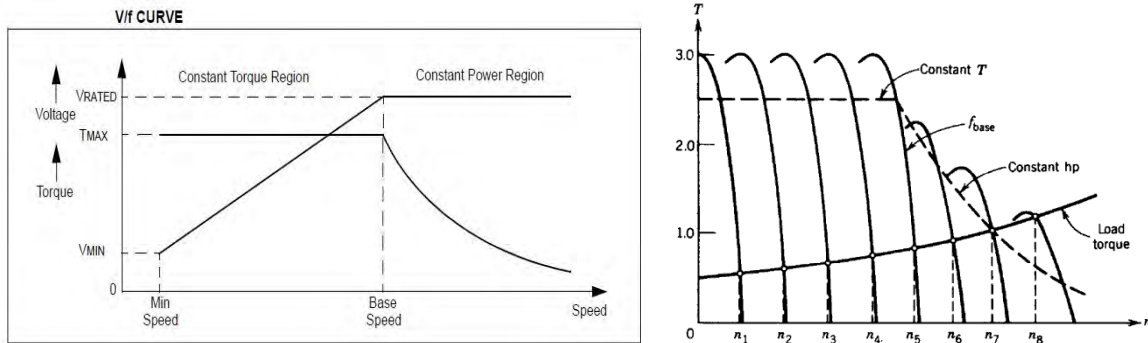


Fig. 25V/F curve

We can conclude easily that it is quadratic with the voltage and not that easily with the slip, as we saw in the previous chapter of this thesis. Thus, if we want to keep the high torque request by heavy deliver vehicles and keep a reasonable speed for such a small kind of vehicles in order to keep it able to cover distances between the supplying center and the customer, we must increase the number of phases and this way, increase the torque provided.

On the right, the V/F curve shows relation with the flux and consequently the torque. So for the purpose that concerns us, with the same  $V_{max}$  and the implementation of more phases, we can reach a higher value of  $T_{max}$  for the same speed limit before the drop of flux. On the left, we can appreciate the curves family corresponding to different points of operation for frequencies with the limitation of voltage shown as a the drop in size. Of course a deep research on speed regulation is not the aim of this thesis so we are not extending more on the techniques used for that purpose.

With the previous considerations we must design a motor with the following characteristics:

- Rated operation conditions      Permanen(S1)
- Indicated power                       $P_{2N} := 55000 \cdot W$
- Number of pole pairs                 $p := 3 \quad 2 \cdot p = 6$
- Phase voltage                           $U_{1N} := 80 \cdot V$
- Phase voltage of the network         $\frac{\Delta}{Y}$
- Frequency                               $f_1 := 50 \cdot Hz$
- Number of stator phases               $m_1 := 6$
- Type of rotor                          Squirrel cage
- Construction of the rotor            1M1001
- Protection class                      IP44
- Cooling                                 ICO141
- Climate conditions and location      N2 – N4

The phases must be symmetrically shifted 60 degrees between phases. Numerous studies demonstrate the advantages of 30 degrees shift between phases in six phases motors in order to minimize the spatial harmonics and get better result in general, but as we will see in calculations, the power requirements (55000W), throw as a number of 72 slots in the stator. Making some calculations, we reach to the conclusion that we can not reach the exact of number slots if we use the shift of 30 degrees, that would mean a stator of 12 poles, making unused some of the slots. Consequently we decided a symmetric distribution of phases and use the complete of the stator slots with a  $q=2$ (slots per phase per pole).

## Methodology

The methodology of working has been divided in two phases:

- Customer stage:
  - ✓ Knowing all the needs and requirements presented by customer
  - ✓ Investigation and researchment regarding the topic and its context
  - ✓ Presentation of a possible solution
- Designing stage
  - ✓ Documentation about all the legislations and standards concerning the project
  - ✓ Development of theoretical model with the implementation in Mathcad
  - ✓ Calculations are send to the industry and wait for the first prototype of the model for later conclusion and improvement from it.(Not achieved by the time I am finishing these thesis)

# Calculations:

---

## 1. Specifications

1. Rated operation conditions	Permanen(S1)
2. Indicated power	$P_{2N} := 55000 \cdot W$
3. Number of pole pairs	$p := 3 \quad 2 \cdot p = 6$
4. Phase Voltage	$U_{1N} := 80 \cdot V$
5. Phase voltage of the network	$\frac{\Delta}{Y}$
6. Frequency	$f_1 := 50 \cdot Hz$
7. Number of stator phases	$m_1 := 6$
8. Type of rotor	Squirrel cage
9. Construction of the rotor	1M1001
10. Protection class	IP44
11. Cooling	ICO141
12. Climate conditions and location	N2 – N4

\*Note: All the used diagrams and tables (Lent. and Pav.) are listed in the appendix, included at the end of the document.

## 2. Magnetic circuits and windings

### 2.1 Size of stator and rotor magnetic circuits

1. According to  $P_{2N}$  and  $2p$ , the nearest standard height of rotation axis is chosen(P.1 lent.):

$$h := 250 \cdot 10^{-3} \cdot m$$

2. External diameter of stator magnetic circuit(P.2 lent.):

$$D_{j1} := 452 \cdot 10^{-3} \cdot m$$

Isotropic electrical steel of 0.5 mm type 2013 is chosen for magnetic circuits because of plates malleability.

Magnetic circuit fill factor  $k_{Fe} := 0.97$

3. Ratio of stator magnetic circuit internal and external diameters plane(P.1 pav.):

$$\frac{D_1}{D_{j1}} = k_D \quad \text{Priimama} \quad k_D := 0.73$$

4. Ratio of stator magnetic circuit internal diameter

$$D_{j1} := D_1 \cdot k_D = 329.96 \times 10^{-3} \text{ m} \quad \text{Imama} \quad D_1 := 330 \times 10^{-3} \text{ m}$$

5. Air gap(P.2 pav.):

$$\delta := 0.7 \cdot 10^{-3} \text{ m}$$

6. External diameter of rotor magnetic circuit

$$D_{j2} := D_1 - 2\delta = 328.6 \times 10^{-3} \text{ m}$$

7. Factor  $k_E$ (P.3 pav.):

$$k_E := 0.98$$

8. Efficiency factor(P.4 pav.):

$$\eta := 0.92$$

9. Power factor(P.5 pav.):

$$\cos\phi := 0.895$$

10. Design power

$$P_{j1}' := \frac{k_E \cdot P_{2N}}{\eta \cdot \cos\phi} = 65.46029 \times 10^3 \text{ W}$$

11. Rotational speed of stator magnetic field

$$n_1 := \frac{f_1}{p} = 16.667 \text{ s}^{-1}$$

12. Mean saturation factor of tooth zone

$$k_z := 1.36$$

\*Approximate value of  $k_z$  is from 1.2 to 1.6. Higher value, for motors of larger power.

13. Pole arc factor (P.6 pav.):

$$\alpha_{\delta} := 0.726$$

14. Field shape factor (P.6 pav.):

$$k_B := 1.088$$

15. Air gap flux density (P.7 pav.):

$$B_{\delta} := 0.7 \cdot T$$

16. Stator linear load (P.8pav.):

$$A_1 := 360 \cdot 10^2 \cdot \frac{A}{m}$$

17. Stator winding and slot:

2) Windings - one layer , build-in; slots – trapezoidal, half closed.

18. Number of stator slots for one pole and phase (P.3 lent. Only for 3 phases):

$$q_1 = \frac{Z_1}{2 \cdot p \cdot m} \quad q_1 := 2$$

19. Stator winding factor (P.4 lent.):

$$k_{w1} := 0.935$$

20. Design length of stator magnetic circuit

$$l_{\delta} := \frac{P'_1}{\pi^2 \cdot \alpha_{\delta} \cdot k_B \cdot k_{w1} \cdot B_{\delta} \cdot A_1 \cdot D_1^2 \cdot n_1} = 196.347 \times 10^{-3} \text{ m} \quad l_{\delta} := 196 \times 10^{-3} \text{ m}$$

21. Geometrical dimensions ratio

$$\lambda_1 := \frac{l_{\delta}}{D_{j1}} = 0.4336$$

\*Maximum ratio (P.9 pav.):

Calculated value compared with  $\lambda_{\max} := 0.77$

$$\lambda_{\max}: \left| \frac{\lambda_{\max} - \lambda_1}{\lambda_{\max}} \cdot 100 \right| = 43.7\%$$

\*Permissible deviation is up to 25% (for optimal length) and up to 60% (for others)

22. Factor  $k_v$  :  $k_v := 0.23$

23. Internal diameter of rotor magnetic circuit

$$D_2 := k_v \cdot D_{j1} = 103.96 \times 10^{-3} \text{ m} \qquad D_2 := 104 \times 10^{-3} \text{ m}$$

## 2.2. Stator winding

24. Number of stator slots

$$Z_1 := 2 \cdot p \cdot m_1 \cdot q_1 = 72$$

25. Relative winding span

For one-layer winding (P.4 lent.)  $\beta := 0.833$

26. Stator winding span (in slots number)

$$y_{n1} := \beta \cdot \frac{Z_1}{2 \cdot p} = 9.996 \qquad \tau_- := \frac{Z_1}{2 \cdot p} = 12$$

27. Indicated phase stator winding current

$$I_{1N} := \frac{P_{2N}}{m_1 \cdot U_{1N} \cdot \eta \cdot \cos\phi} = 139.159 \text{ A}$$

28. Stator slots pitch

$$t_1 := \frac{\pi \cdot D_1}{Z_1} = 14.399 \times 10^{-3} \text{ m}$$

29. Effective number of conductors in stator slot

$$\text{if } a_1 := 1 \qquad N_{n1} := \frac{A_1 \cdot t_1 \cdot a_1}{I_{1N}} = 3.725 \qquad N_{n1} := 4$$

30. Stator winding current density (P.12 pav.):

$$J_1 := 5 \cdot 10^6 \cdot \frac{\text{A}}{\text{m}^2}$$

31. Cross section area of non-isolated conductor from

$$\text{If } N_{e11} := 16 \qquad q := \frac{I_{1N}}{a_1 \cdot N_{e11} \cdot J_1} = 1.739 \times 10^{-6} \text{ m}^2$$

Cross section of the conductor is chosen according to these recommendations: when  $h \leq 132$  mm, maximum diameter of isolated conductor  $d_{1\max} = 1.33$  mm; when  $h \geq 160$  mm,  $d_{1\max} = 1.685$  mm. Diameters of non-isolated conductors are found:  $d_{\min} = 1.25$  mm,  $d_{\max} = 1.60$  mm, and corresponding cross section areas  $q_{\min} = 1.277 \text{ mm}^2$  and  $q_{\max} = 2.011 \text{ mm}^2$ .

At first, we calculate for  $a_1 = 1$  and  $N_{e11} = 1$ . If  $q \leq q_{\max}$ , calculation is stopped. When  $q > q_{\max}$ ,  $N_{e11}$  is increased up to permissible value ( $2p \geq 4 - N_{e11} = 6-8$ ,  $2p = 2 - N_{e11} = 8-9$ ), while  $q \leq q_{\max}$ . If we get  $q > q_{\max}$ , the

number of parallel branches  $a_1$  should be increased. Number of parallel branches should be multiple of pole number  $2p$ .

The nearest standard cross section area of non-isolated conductor is chosen (P.5 lent.):

$$q := 1.767 \cdot 10^{-6} \cdot \text{m}^2 < q_{\max}, \quad q_{\max} = 2.011 \times 10^{-6} \text{m}^2$$

Rated diameter of non-isolated conductor

$$d := 1.5 \cdot 10^{-3} \cdot \text{m}$$

Internal diameter of isolated conductor

$$d_1 := 1.585 \cdot 10^{-3} \cdot \text{m}$$

Insulation class (P.6 lent.)  $\rightarrow$  **F**

32. Actual current density of stator winding

$$J_1 := \frac{I_{1N}}{N_{e11} \cdot a_1 \cdot q} = 5 \times 10^6 \text{A} \cdot \text{m}^{-2}$$

Comparison with chosen value

$$\left| \frac{J_1 - J_{1.}}{J_{1.}} \right| \cdot 100 = 0 \%$$

\*Permissible deviation up to 10 %.

33. Number of stator winding phase serial turns

$$w_1 := \frac{N_{n1}}{a_1} \cdot p \cdot q_1 = 24$$

34. Actual linear load of stator

$$A_1 := \frac{2 \cdot I_{1N} \cdot w_1 \cdot m_1}{\pi \cdot D_1} = 38.658 \times 10^3 \text{A} \cdot \text{m}^{-1}$$

Comparison with chosen value

$$\left| \frac{A_1 - A_{1.}}{A_{1.}} \right| \cdot 100 = 7.38\%$$

\*Permissible deviation up to 10 %

35. Winding thermal characteristic (P.13 pav.):

$$A_{1J1} := 1800 \cdot 10^8 \cdot \frac{\text{A}^2}{\text{m}^3}$$

$$A_1 \cdot J_1 = 193.29 \times 10^9 \text{A}^2 \cdot \text{m}^{-3}$$

Comparison

$$\left| \frac{A_{1J1} - A_1 \cdot J_1}{A_{1J1}} \right| \cdot 100 = 7.383 \%$$

\*Permissible deviation up to 20 %

36. Stator winding distribution factor

$$k_{d01} := \frac{0.5}{q_1 \cdot \sin\left(\frac{\pi}{6 \cdot q_1}\right)} = 0.96593$$

37. Stator winding span decrease factor

$$k_{\beta 1} := \sin\left(\beta \cdot \frac{\pi}{2}\right) = 0.966$$

38. Stator winding factor

$$k_{w1} := k_{d01} \cdot k_{\beta 1} = 0.93288$$

\*Also showed results in P.4 lent

39. Motor air gap magnetic flux

$$\Phi_{\delta} := \frac{k_E \cdot U_{1N}}{4 \cdot k_B \cdot k_{w1} \cdot w_1 \cdot f_1} = 16.092 \times 10^{-3} \text{ Wb}$$

40. Pole pitch

$$\tau := \frac{\pi \cdot D_1}{2 \cdot p} = 172.788 \times 10^{-3} \text{ m}$$

41. Actual motor air gap magnetic flux

$$B_{\delta} := \frac{\Phi_{\delta}}{\alpha_{\delta} \cdot \tau \cdot l_{\delta}} = 0.655 \text{ T}$$

Comparison with chosen value

$$\left| \frac{B_{\delta} - B_{\delta}}{B_{\delta}} \right| \cdot 100 = 6.951 \%$$

\*Permissible deviation up to 10 %



### 2.3. Dimensions of stator slot, tooth, yoke and winding

42. Stator slots: Trapezoid, semi closed, tooth walls parallel

43. Trapezoid dimensions:

$$D_1 = 330 \times 10^{-3} \text{ m}$$

$$t_1 = 0.0144 \text{ m}$$

$$D_{j1} = 452 \times 10^{-3} \text{ m}$$

$$t'_1 := t_1 \cdot \frac{D_{j1}}{D_1} = 19.722 \times 10^{-3} \text{ m} \quad h'_1 := \frac{D_{j1} - D_1}{2} = 61 \times 10^{-3} \text{ m}$$

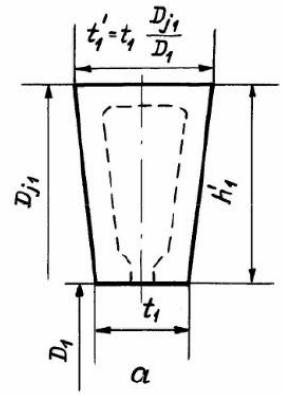


Fig. 26 Stator trapezoid dimensions

44. Stator yoke magnetic flux density(P.7 lent.):

Chosen value 0.25 T

45. Stator tooth magnetic flux density(P.8 lent.):

Chosen value 0.715 T

46. Stator yoke height

$$h_{j1} := \frac{\Phi_{\delta}}{2 \cdot l_{\delta} \cdot k_{Fe} \cdot B_{j1}} = 31.349 \times 10^{-3} \text{ m}$$

47. Stator tooth width

$$b_{z1} := \frac{B_{\delta} \cdot t_1}{k_{Fe} \cdot B_{z1}} = 5.813 \times 10^{-3} \text{ m}$$

48. Stator slot dimensions (P.9 lent.):

$$h_{s1} := 1.0 \cdot 10^{-3} \cdot \text{m} \quad b_{s1} := 3.7 \cdot 10^{-3} \cdot \text{m}$$

and  $r_1 := 1.0 \cdot 10^{-3} \cdot \text{m} \quad \beta_g := 45^\circ \quad \beta_g = 0.785 \text{ rad}$

From the drawing, slot dimensions are:

$$h_{n1} := h'_1 - h_{j1} = 29.651 \times 10^{-3} \text{ m}$$

$$b_1 := 12.6 \cdot 10^{-3} \cdot \text{m} \quad b_2 := 9.6 \cdot 10^{-3} \cdot \text{m} \quad h_3 := 2.8 \cdot 10^{-3} \cdot \text{m}$$

49. Stator slot dimensions tolerance, taking into account magnetic circuit assembly errors(P.10 lent.):

$$\Delta b_s := 0.2 \cdot 10^{-3} \cdot \text{m} \quad \Delta h_s := 0.2 \cdot 10^{-3} \cdot \text{m}$$

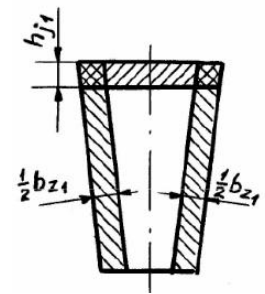


Fig. 27 Stator tooth dimension

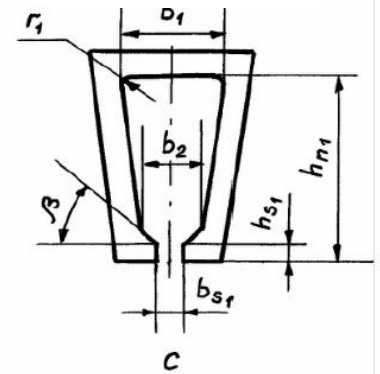


Fig. 28 Stator slot dimensions

50. Stator slot cross section area in stamp:

$$Q_{n1} := \frac{b_1 + b_2}{2} \cdot \left( h_{n1} - h_{s1} - \frac{b_2 - b_{s1}}{2} \right) = 285.278 \times 10^{-6} \text{ m}^2$$

51. Corrected cross section of assembled stator magnetic circuit

$$Q'_{n1} := \left( \frac{b_1 + b_2}{2} - \Delta b_s \right) \cdot \left( h_{n1} - h_{s1} - \frac{b_2 - b_{s1}}{2} - \Delta h_s \right) = 277.9577 \times 10^{-6} \text{ m}^2$$

52. Insulation of stator winding slot (P. 11 lent.):

Insulation class F

53. Thickness of stator slot insulation (P. 12 lent.):

$$b_i := 0.4 \cdot 10^{-3} \text{ m}$$

54. Cross section area of stator slot insulation

$$Q_i := b_i \cdot (2 \cdot h_{n1} + b_1 + b_2) = 32.601 \times 10^{-6} \text{ m}^2$$

55. Cross section area of stator slot streak and closing insulation (P. 13 lent.):

$$2) \quad Q_t := 0.4 \text{ m} \cdot b_1 \cdot 10^{-3} + 0.9 \text{ m} \cdot b_2 \cdot 10^{-3} = 13.68 \times 10^{-6} \text{ m}^2$$

56. Cross section area of winding in stator slot

$$Q_{n1f} := Q'_{n1} - Q_i - Q_t = 231.677 \times 10^{-6} \text{ m}^2$$

57. Filling factor of stator slot  $k_{Cu1}$ :

$$N_{n1} = 4 \qquad d_1 = 1.585 \times 10^{-3} \text{ m} \qquad N_{el1} = 16$$

$$k_{Cu1} := \frac{N_{n1} \cdot N_{el1} \cdot d_1^2}{Q_{n1f}} = 0.694$$

$k_{Cu1}$  Recommended **0.68 - 0.75**.

When  $k_{Cu} < 0.68$ , slot area should be decreased by increasing  $b_{z1}$  and/or  $h_{j1}$ . In this case, magnetic flux density of stator tooth and yoke decreases. If  $B_{z1}$  and  $B_{j1}$  need to be decreased even more, the motor design is wrong. In such case, length of stator magnetic circuit or height  $h$  should be less.

When  $k_{Cu1} > 0.75$ , the  $b_{z1}$  and/or  $h_{j1}$  should be decreased. If  $k_{Cu1}$  is higher than recommended at maximum permissible  $B_{z1}$  and  $B_{j1}$ , length of stator magnetic circuit or height  $h$  should be higher.

After  $k_{Cu1}$  correspond requirements, the final dimensions of stator slot and tooth are corrected.

58. Mean pitch of stator slots:

$$t_{1vid} := \frac{\pi \cdot (D_1 + h_{n1})}{Z_1} = 15.693 \times 10^{-3} \text{ m}$$

59. Mean area of stator winding coil

$$b_{ar1} := t_{1vid} y_{n1} = 156.864 \times 10^{-3} \text{ m}$$

60. Mean estimated length of stator winding overhead

$$L_{s1} := (1.16 + 0.14 \cdot p) \cdot b_{ar1} + 15 \cdot 10^{-3} \cdot \text{m} = 262.846 \times 10^{-3} \text{ m}$$

61. Mean length of stator turn

$$L_{ar1} := 2 \cdot (l_{\delta} + L_{s1}) = 917.692 \times 10^{-3} \text{ m}$$

62. Height of stator winding overhead

$$2) \quad h_{g1} := (0.12 + 0.15 \cdot p) \cdot b_{ar1} + 10 \cdot 10^{-3} \cdot \text{m} = 99.413 \times 10^{-3} \text{ m}$$

Pitch angle of winding overhead

$$\alpha_{g1} := 0.12 \text{ rad}$$

#### 2.4. Dimensions of rotor slot, tooth, yoke and winding

63. Rotor slots number (P.14 lent.):

$$Z_2 := 56$$

64. Rotor slot: (P.15 pav.): - Oval, semi-closed

65. Pitch of rotor slots

$$t_2 := \frac{\pi \cdot D_{j2}}{Z_2} = 18.434 \times 10^{-3} \text{ m}$$

66. Trapezoid dimensions:

$$D_{j2} = 328.6 \times 10^{-3} \text{ m} \quad D_2 = 104 \times 10^{-3} \text{ m} \quad t_2 = 18.434 \times 10^{-3} \text{ m}$$

$$h'_2 := \frac{D_{j2} - D_2}{2} = 112.3 \times 10^{-3} \text{ m}$$

$$t'_2 := t_2 \cdot \frac{D_2}{D_{j2}} = 5.834 \times 10^{-3} \text{ m}$$

67. Rotor slot height (P.17 pav.):

$$h_{n2} := 40 \cdot 10^{-3} \text{ m}$$

68. Rotor tooth magnetic flux density:

$$B_{z2} := 1.5545 \text{ T}$$

69. Rotor tooth width

$$b_{z2} := \frac{t_2 \cdot B_\delta}{k_{Fe} \cdot B_{z2}} = 8.002 \times 10^{-3} \text{ m}$$

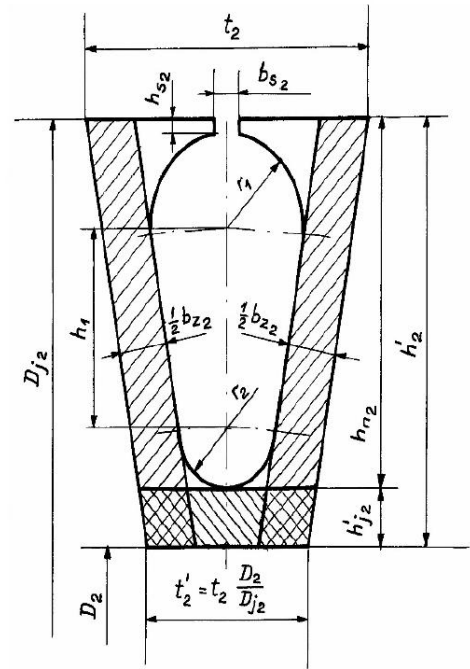


Fig. 29 Rotor trapezoid dimensions

70. Rotor slot dimensions

$$h_{s2} := 0.7 \cdot 10^{-3} \text{ m} \quad b_{s2} := 1.5 \cdot 10^{-3} \text{ m} \quad h_2 := 0.3 \cdot 10^{-3} \text{ m}$$

From drawing, the rotor slot dimensions are obtained

$$r_{1r} := 4.75 \cdot 10^{-3} \text{ m} \quad r_{2r} := 2.6 \cdot 10^{-3} \text{ m} \quad h_{1r} := 32.25 \cdot 10^{-3} \text{ m}$$

$$h'_{j2} := h'_2 - h_{n2} = 72.3 \times 10^{-3} \text{ m}$$

71. Design height of rotor yoke

$$h_{j2} := \frac{2+p}{3.2p} \cdot \left( \frac{D_{j2}}{2} - h_{n2} \right) = 64.74 \times 10^{-3} \text{ m}$$

72. Magnetic flux density of rotor yoke

$$B_{j2} := \frac{\Phi_\delta}{2 \cdot l_\delta \cdot k_{Fe} \cdot h_{j2}} = 653.72 \times 10^{-3} \text{ T}$$

\*Calculated  $B_{j2}$  does not exceed permissible value (P.16 lent.) 1.15 T.

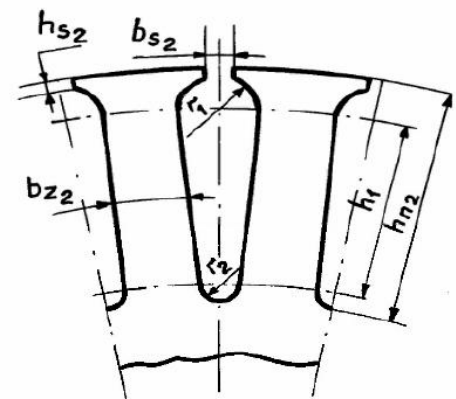


Fig. 30 Rotor slot dimensions

73. Cross section area of rotor squirrel cage winding bar

$$Q_{n2} := \frac{\pi}{2} \cdot (r_{1r}^2 + r_{2r}^2) + (r_{1r} + r_{2r}) \cdot h_{1r} = 283.097 \times 10^{-6} \text{ m}^2$$

$$q_{cr} := Q_{n2} \quad q_{cr} = 283.097 \times 10^{-6} \text{ m}^2$$

74. Current of rotor squirrel cage winding bar

When  $\cos\phi = 0.895$  so  $k_I := 0.94$  (P18 pav.)

$$I_c := k_I \cdot I_{1N} \cdot \frac{6 \cdot w_1 \cdot k_{w1}}{Z_2} = 313.79 \text{ A}$$

75. Current density of rotor squirrel cage bar:

$$J_c := \frac{I_c}{q_{cr}} = 1.108 \times 10^6 \text{ A} \cdot \text{m}^{-2}$$

\*Recommended current density  $2 \cdot 10^6$  to  $4.5 \cdot 10^6$

76. Rotor slot skewing:

$$\frac{1}{Z_1} = 0.014 \quad \frac{b_{s2}}{\pi \cdot D_1} = 0.001$$

77. Rotor cage ring dimensions (P. 19 pav.):

Ring height:

$$h_z := 1.28 \cdot h_{n2} = 51.2 \times 10^{-3} \text{ m}$$

Cross section area:

$$q_z := 0.375 \cdot \frac{Z_2 \cdot q_{cr}}{2 \cdot p} = 990.84 \times 10^{-6} \text{ m}^2$$

Ring length:

$$L_z := \frac{q_z}{h_z} = 19.352 \times 10^{-3} \text{ m}$$

Mean ring diameter

$$D_{zvid} := D_{j2} - h_z = 277.4 \times 10^{-3} \text{ m}$$

78. Current Rotor cage ring:

$$I_z := I_c \cdot \frac{1}{2 \cdot \sin\left(\frac{\pi \cdot p}{Z_2}\right)} = 936.653 \text{ A}$$

79. Current density of Rotor cage ring

$$J_z := \frac{I_z}{q_z} = 945.312 \times 10^3 \text{ A} \cdot \text{m}^{-2}$$

\*Recommended current density of cage ring:

$$0.6 J_c = 665.051 \times 10^3 \text{ A} \cdot \text{m}^{-2}$$

$$0.92 J_c = 1.02 \times 10^6 \text{ A} \cdot \text{m}^{-2}$$

## 2.5. Calculation of magnetic circuit. Magnetizing current.

80. Factor evaluating dentation of stator:

$$k_{n1} := 1 + \frac{b_{s1}}{t_1 - b_{s1} + \frac{5 \cdot \delta \cdot t_1}{b_{s1}}} = 1.152$$

81. Factor evaluating dentation of rotor:

$$k_{n2} := 1$$

Rotor slot is open without skewing.

82. Air gap factor:  $k_\delta := k_{n1} \cdot k_{n2} = 1.152$

83. Magnetic potential difference of pole pair air gap:

$$F_\delta := 1.6 \cdot \delta \cdot k_\delta \cdot B_\delta \cdot 10^6 \cdot (\text{kg}^{-1} \cdot \text{s}^2 \cdot \text{m}^{-1} \cdot \text{A}^2) = 844.574 \text{ A}$$

84. Magnetic field strength of stator teeth (P.17 lent.):

$$\text{When } H_{z1} := 34 \cdot 10^2 \cdot \frac{\text{A}}{\text{m}} \quad B_{z1} = 1.671 \text{ T}$$

85. Design length of stator teeth magnetic lines:

$$L_{z1} := h_{n1} \quad L_{z1} = 29.651 \times 10^{-3} \text{ m}$$

86. Magnetic potential difference of stator teeth:

$$F_{z1} := 2 \cdot L_{z1} \cdot H_{z1} = 201.625 \text{ A}$$

87. Design length of rotor teeth magnetic lines:

$$L_{z2} := h_{n2} - 0.2 \cdot r_{2r} = 39.48 \times 10^{-3} \text{ m}$$

88. Magnetic field strength of rotor teeth (P.17 lent.):

$$\text{When } H_{z2} := 11.310^2 \cdot \frac{\text{A}}{\text{m}} \quad B_{z2} = 1.555 \text{ T}$$

89. Magnetic potential difference of rotor teeth:

$$F_{z2} := 2 \cdot L_{z2} \cdot H_{z2} = 89.225 \text{ A}$$

90. Saturation factor of tooth zone:

$$k_{z..} := \frac{F_{\delta.} + F_{z1.} + F_{z2.}}{F_{\delta.}} = 1.344$$

\*But initial pole arc factor: gave us  $k_{z.} = 1.36$        $\alpha_{\delta} = 0.726$

\*According to calculated factor  $kz=1.334$  we find now from (P.6pav.)  $\alpha'_{\delta} := 0.725$

91. Factor of magnetic flux density change:

$$k_a := \frac{\alpha_{\delta}}{\alpha'_{\delta}} = 1.00138$$

\*If the change exceeds 0.01, magnetic flux strengths and magnetic potential differences should be recalculated

$$|1 - k_a| = 0.0014$$

92. Corrected values of magnetic fluxes, magnetic field strengths and magnetic potential differences (in this case there was no need to recalculate anyway)

$$B_{\delta-} := B_{\delta} \cdot k_a = 0.655 \text{ T}$$

$$F_{\delta.} = 844.574 \text{ A}$$

$$k_{z..} = 1.344$$

$$k_{1.} := \frac{\text{A}}{\text{m}}$$

$$k_{2.} := \frac{\text{A}}{\text{m}}$$

$$B_{z1} := B_{z1.} \cdot k_a = 1.674 \text{ T}$$

$$H_{z1..} := k_{1.} \cdot 47.010^2 = 4.7 \times 10^3 \text{ A} \cdot \text{m}^{-1}$$

$$B_{z2} := B_{z2.} \cdot k_a = 1.557 \text{ T}$$

$$H_{z2.} := k_{2.} \cdot 14.610^2 = 1.46 \times 10^3 \text{ A} \cdot \text{m}^{-1}$$

$$F_{z1} := 2 \cdot L_{z1} \cdot H_{z1..} = 278.717 \text{ A}$$

$$F_{z2} := 2 \cdot L_{z2} \cdot H_{z2.} = 115.282 \text{ A}$$

93. Design length of stator yoke magnetic lines:

$$L_{j1} := \frac{(D_{j1} - h_{j1}) \cdot \pi}{2 \cdot p} = 220.252 \times 10^{-3} \text{ m}$$

94. Stator yoke magnetic field strength (P.17 lent.):

$$H_{j1} := 1.25 \cdot 10^2 \cdot \frac{\text{A}}{\text{m}}$$

According to

$$B_{j1} := B_{j1} - 0.4 \cdot T = 950 \times 10^{-3} \text{ T}$$

95. Stator yoke magnetic potential difference:

$$F_{j1} := H_{j1} \cdot L_{j1} = 27.532 \text{ A}$$

96. Design length of rotor yoke magnetic lines:

$$L_{j2} := \frac{\pi \cdot (D_2 + h_{j2})}{2 \cdot p} = 88.352 \times 10^{-3} \text{ m}$$

97. Rotor yoke magnetic field strength (P.17 lent.):

According to  $H_{j2} := 1.21 \cdot 10^2 \cdot \frac{\text{A}}{\text{m}}$   $B_{j2} = 653.72 \times 10^{-3} \text{ T}$   $\xi := 0.525$  **Figure 29**

98. Rotor yoke magnetic potential difference:

$$F_{j2} := \xi \cdot H_{j2} \cdot L_{j2} = 5.613 \text{ A}$$

99. Pole pair magneto motive force:

$$F_{\Sigma} := F_{\delta} + F_{z1} + F_{z2} + F_{j1} + F_{j2} = 1.272 \times 10^3 \text{ A}$$

100. Saturation factor of magnetic circuit:

$$k_s := \frac{F_{\Sigma}}{F_{\delta}} = 1.506$$

101. Magnetising current:

$$I_m := \frac{p \cdot F_{\Sigma}}{0.9 \cdot m_1 \cdot w_1 \cdot k_{w1}} = 31.556 \text{ A}$$

Relative magnetising current in percent:

$$i_m := \frac{I_m}{I_{1N}} \cdot 100 = 22.676\%$$

\*Usual relative magnetising current in percent 37 - 75 %. So we have here one of the best parameters achieved with this steel.



## 2.6. Motor operating conditions parameters

### 2.6.1. Resistances of stator and rotor windings

102. Specific electrical conductance of stator winding:

$$\gamma_{\theta} := 41 \cdot 10^6 \cdot \frac{\text{S}}{\text{m}} \quad \text{Insulation class F}$$

\*We are taking common industrial copper characteristic from standards.

103. Resistance of stator winding phase:

$$R_1 := \frac{1}{\gamma_{\theta}} \cdot \frac{w_1 \cdot L_{ar1}}{a_1 \cdot N_{el1} \cdot q} = 0.0193 \Omega$$

In per units:

$$R^*_1 := \frac{I_{1N} \cdot R_1}{U_{1N}} = 0.03357$$

Resistance in per units of stator winding phase of induction motors of analysed power is: 0.037 - 0.22 pu. Higher values for motors of smaller power

104. Specific electrical conductance of rotor cage winding (P18 lent.):

Insulation class F

$$\gamma'_{\theta} := 20.5 \cdot 10^6 \cdot \frac{\text{S}}{\text{m}}$$

105. Resistance of rotor cage bar

$$R_c := \frac{l_{\delta}}{\gamma'_{\theta} \cdot q_{cr}} = 33.773 \times 10^{-6} \Omega$$

\*angle calculated with (76)

106. Resistance of rotor cage ring part between next bars:

$$R_z := \frac{\pi \cdot D_{zvid}}{\gamma'_{\theta} \cdot Z_2 \cdot q_z} = 766.145 \times 10^{-9} \Omega$$

107. Resistance of rotor cage winding phase:

$$R_2 := R_c + \frac{R_z}{2 \cdot \sin\left(\frac{\pi \cdot p}{Z_2}\right)^2} = 47.425 \times 10^{-6} \Omega$$

108. Factor of rotor winding parameters reduction:

$$k_{r1} := \frac{4 \cdot m_1 \cdot (w_1 \cdot k_{w1})^2}{Z_2} = 214.832$$

109. Reduced resistance of rotor winding phase:

$$R'_2 := R_2 \cdot k_{r1} = 10.189 \times 10^{-3} \Omega$$

In per units:

$$R'^*_2 := \frac{I_{1N} \cdot R'_2}{U_{1N}} = 0.01772$$

\*Reduced resistance in per units of rotor cage winding of induction motors of analysed power is: - 0.016 - 0.23 pu. Higher values for motors of smaller power.

## 2.6.2. Leakage reactance and reactance of mutual inductance of stator and rotor windings

110. Factors (P.21 pav)

When  $\beta = 0.833$

$$k_\beta := 0.906 \quad k'_\beta := 0.875$$

111. Winding height in the slot:

$$h_1 := h_{n1} - h_{s1} - h_3 - b_i = 25.451 \times 10^{-3} \text{ m}$$

\*Thickness of slot insulation  $b_i = 4 \times 10^{-4} \text{ m}$

112. Relative leakage magnetic conductance of stator trapezoidal slot:

$$\lambda_{n1} := \frac{h_1}{3 \cdot b_2} \cdot k_\beta + \left( \frac{3 \cdot h_3}{b_2 + 2 \cdot b_{s1}} + \frac{h_{s1}}{b_{s1}} \right) \cdot k'_\beta = 1.469$$

113. Factor  $k_{d1}$ , estimating damping response of currents injected by stator field higher order harmonics in rotor cage winding (P.19 lent.):

$$\frac{Z_2}{p} = 18.667 \quad q_1 = 2 \quad k_{d1} := 0.778$$

114. Factor  $k_{s1}$ , estimating effect of stator slots rips:

$$k_{s1} := 1 - 0.033 \frac{b_{s1}^2}{t_1 \cdot \delta} = 0.955$$

115. Factor of stator differential leakage (P.20 lent)

$$\text{When } q_1 = 2 \quad \beta = 0.833 \quad k_{y1} := \frac{Z_1}{2 \cdot p} - \beta \cdot \frac{Z_1}{2 \cdot p} = 2.004$$

$$k'_{d1} := 0.0062$$

116. Relative magnetic conductance of differential leakage

$$\lambda_{d1} := \frac{0.9 \cdot t_1 \cdot (q_1 \cdot k_{w1})^2 \cdot k_{d1} \cdot k_{s1} \cdot k'_{d1}}{\delta \cdot k_{\delta}} = 257.715 \times 10^{-3}$$

117. Relative magnetic conductance of stator winding overhand leakage:

$$\lambda_{s1} := 0.34 \frac{q_1}{l_{\delta}} \cdot (L_{s1} - 0.64 \beta \cdot \tau) = 0.592$$

118. Relative magnetic conductance of stator winding leakage per winding:

$$\Lambda_1 := \lambda_{n1} + \lambda_{d1} + \lambda_{s1} = 2.32$$

119. Reactance of stator winding phase (without skewing of slots):

$$k_{X1} := 1.58 \cdot 10^{-5} \cdot m^{-1} \cdot s \cdot \Omega$$

$$X_1 := \frac{k_{X1} \cdot f_1 \cdot w_1^2 \cdot l_{\delta}}{p \cdot q_1} \cdot \Lambda_1 = 0.034 \Omega$$

In per units:

$$X^*_1 := \frac{I_{1N} \cdot X_1}{U_{1N}} = 0.06$$

\*Reactance of stator winding phase is: 0.1 - 0.18 pu. higher values for motors of smaller power.

120. Relative magnetic conductance of rotor slot leakage:

$$k_{Ic} := I_c \cdot A^{-1} \cdot m$$

$$\lambda_{n2} := \frac{h_{1r} + 0.8 \cdot r_{2r}}{6 \cdot r_{1r}} \cdot \left( 1 - \frac{\pi \cdot r_{1r}}{2 \cdot q_{cr}} \right)^2 + 0.66 - \frac{b_{s2}}{4 \cdot r_{1r}} + 0.3 + \frac{1.12 \cdot h_2 \cdot 10^6}{k_{Ic}} = 2.874$$

121. Factor of rotor differential leakage (P.22 pav.):

$$\text{When } q_2 := \frac{Z_2}{2 \cdot p \cdot m_1} = 1.556 \text{ so } k'_{d2} := 0.0093$$

122. Relative magnetic conductance of rotor differential leakage:

$$\lambda_{d2} := \frac{0.9 \cdot t_2 \cdot \left( \frac{Z_2}{2 \cdot p \cdot m_1} \right)^2 \cdot k'_{d2}}{\delta \cdot k_\delta} = 462.938 \times 10^{-3}$$

123. Relative magnetic conductance of rotor cage rings leakage:

$$\lambda_z := \frac{2.3 \cdot D_{zvid}}{Z_2 \cdot l_\delta \cdot \left( 2 \cdot \sin \left( \frac{\pi \cdot p}{Z_2} \right) \right)^2} \cdot \log \left( \frac{4.7 \cdot D_{zvid}}{h_z + 2 \cdot L_z} \right) = 0.60153$$

124. Relative magnetic conductance of rotor winding leakage:

$$\Lambda_2 := \lambda_{n2} + \lambda_{d2} + \lambda_z = 3.938$$

125. Reactance of cage rotor winding phase leakage (neglecting diagonal of slots):

$$k_{x2} := 7.9 \cdot m^{-1} \cdot s \cdot \Omega$$

$$X_2 := k_{x2} \cdot f_1 \cdot l_\delta \cdot \Lambda_2 \cdot 10^{-6} = 304.891 \times 10^{-6} \Omega$$

126. Reduced resistance of rotor winding phase leakage

$$X'_2 := X_2 \cdot k_{r1} = 0.066 \Omega$$

In per units:

$$X'^*_{2} := \frac{I_{1N} \cdot X'_2}{U_{1N}} = 0.114$$

\*Reduced relative reactance of rotor winding phase is 0.16 - 0.32 pu. Higher values for motors of smaller power.

127. Mutual reactance (neglecting diagonal of slots)

$$X_m := \frac{U_{1N} - I_m \cdot X_1}{I_m} = 2.501 \Omega$$

In per units:

$$X^*_m := \frac{I_{1N} \cdot X_m}{U_{1N}} = 4.35$$

\*Mutual reactance is: 1.2 - 3.1 pu. higher values for motors of smaller power. If rotor slots are diagonal, reactances of stator and rotor are higher. This is not accounted in previous calculations. Increase of reactances is evaluated by factor  $k_i$ .

128. Central angle of diagonal:

$$\gamma_s := 0 \text{ rad}$$

\*decided not to apply any angle after checking the deference is low

129. Factor  $\epsilon$ :

No need to calculate since the chosen angle of bars is 0.

130. Factor evaluating diagonals of slots (P.21 lent.):  $k_{is} := 1.0$

131. Leakage reactances when diagonal are accounted:

No need to calculate since the chosen angle of bars is 0.

### 3. Magnetic and mechanic losses

132. Stator teeth mass of magnetic field:

$$k_{Gz1} := 7.8 \cdot 10^3 \cdot \text{m}^{-3} \cdot \text{kg} \quad \text{*the chosen steel characteristics}$$

$$G_{z1} := k_{Gz1} \cdot Z_1 \cdot b_{z1} \cdot h_{n1} \cdot \delta \cdot k_{Fe} = 18.402 \text{ kg}$$

133. Stator yoke mass:

$$k_{Gj1} := k_{Gz1} = 7.8 \times 10^3 \text{ m}^{-3} \cdot \text{kg}$$

$$G_{j1} := k_{Gj1} \cdot \pi \cdot (D_{j1} - h_{j1}) \cdot h_{j1} \cdot \delta \cdot k_{Fe} = 61.436 \text{ kg}$$

134. The main magnetic losses of stator teeth:

$$k_{z1} := 4.59 \text{ A}^2 \cdot \text{m}^2 \cdot \text{kg}^{-2} \cdot \text{s} \quad \text{*the chosen steel characteristics}$$

$$p_{z1} := k_{z1} \cdot B_{z1}^2 \cdot G_{z1} = 236.636 \text{ W}$$

135. The main stator yoke losses:

$$k_{j1} := 4.08 \text{ A}^2 \cdot \text{m}^2 \cdot \text{kg}^{-2} \cdot \text{s} \quad \text{*the chosen steel characteristics}$$

$$p_{j1} := k_{j1} \cdot B_{j1}^2 \cdot G_{j1} = 456.825 \text{ W}$$

136. The main magnetic losses:

$$p_{Feh} := p_{z1} + p_{j1} = 693.46 \text{ W}$$

137. Factor  $\beta_0$  (P.23 pav.)

$$\text{When } \frac{b_{s1}}{\delta} = 5.286 \quad \beta_0 := 0.305$$

138. Magnitude of magnetic flux density oscillation:

$$B_0 := \beta_0 \cdot k_{\delta} \cdot B_{\delta} = 0.23 \text{ T}$$

139. Specific losses of rotor surface:

$$k_{s2} := 465 \cdot s^{2.5} \cdot A^2 \cdot m^{-2} \cdot kg^{-1} \quad \text{*the chosen aluminum characteristics}$$

$$\frac{W}{m^2} = 1 \cdot kg \cdot s^{-3} \cdot 1.5 \cdot (B_0 \cdot t_1)^2 = 211.995 \cdot kg \cdot s^{-3}$$

140. Surface losses of rotor teeth:

$$P_{s2} := 2 \cdot p \cdot \tau \cdot \frac{t_2 - b_{s2}}{t_2} \cdot l_{\delta} \cdot p_{s2} = 39.572 W$$

141. Rotor teeth mass:

Irrelevant for our calculations, because frequency of rotor magnetic field is too small in steady state, around 1Hz.

142. Factor  $\gamma_1$ :

Irrelevant for our calculations, because frequency of rotor magnetic field is too small in steady state, around 1Hz.

143. Magnitude of magnetic flux density oscillation:

Irrelevant for our calculations, because frequency of rotor magnetic field is too small in steady state, around 1Hz.

144. Pulsing losses of rotor teeth:

$$P_{p2\_} := 0 \quad \text{Irrelevant for our calculations, because frequency of rotor magnetic field is too small in steady state, around 1Hz.}$$

145. Additional magnetic losses:

$$P_{Fea} := P_{s2} + P_{p2\_} = 39.572 W$$

146. Idle operation magnetic losses:

$$P_{Fe\Sigma} := P_{Feh} + P_{Fea} = 733.032 W$$

147. Factor:

$$k_m := 1 \quad \text{because} \quad 2 \cdot p = 6$$

148. Mechanic losses:

$$k_{m\Sigma} := 36 \cdot m^{-2} \cdot kg \cdot s^{-1}$$

$$P_{m\Sigma} := k_{m\Sigma} \cdot k_m \cdot n_1^2 \cdot D_{j1}^4 = 417.40 W$$

149. Steel resistance:

$$R_m := \frac{P_{Feh}}{m_l \cdot I_m^2} = 116.067 \times 10^{-3} \Omega$$

In per unit:

$$R_m^* := \frac{I_{1N} \cdot R_m}{U_{1N}} = 0.2019$$

\*Relative resistance  $R_m$  pu is - 0.03 - 0.25 pu Higher values for motors of smaller power

150. Angle  $\gamma_1$ :

$$\gamma_1 := \text{atan} \left( \frac{R_1 \cdot X_m - X_1 \cdot R_m}{R_m^2 + X_m^2 + R_1 \cdot R_m + X_1 \cdot X_m} \right) = 0.00696 \text{ rad}$$

151. Factor  $c_1$ :

$$c_1 := \sqrt{\frac{(R_1 + R_m)^2 + (X_1 + X_m)^2}{R_m^2 + X_m^2}} = 1.014$$

## 4. Motor parameters and characteristics

### 4.1. Parameters of equivalent circuit

152. Parameters of equivalent circuit:

$R_1 = 0.019 \Omega$	(103 item)	$R'_2 = 0.01 \Omega$	(109 item)
		$c_1 = 1.014$	
$X_1 = 0.034 \Omega$	(131 item)	$X'_2 = 0.066 \Omega$	(131 item)
$X_m = 2.501 \Omega$	(131 item)	$R_m = 0.116 \Omega$	(149 item)
$\gamma_1 = 0.00696$	rad (150 item)		(151 item)

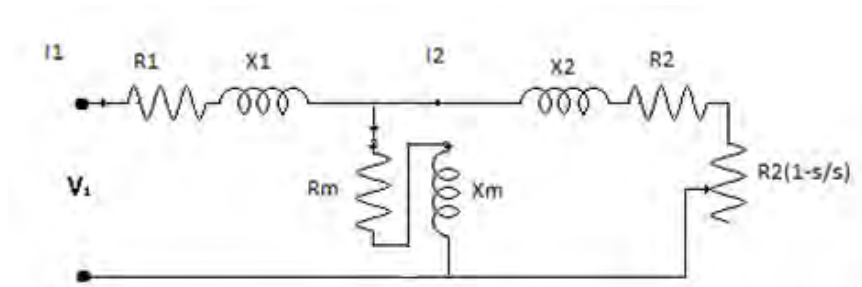


Fig. 31 Equivalent circuit parameters

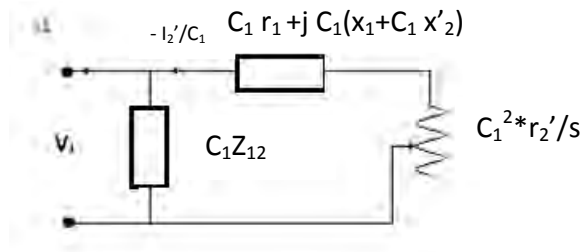


Fig. 32 equivalent circuit transformation

#### 4.2. Start characteristics

153. Motor maximum torque:  $M_m$

$$M_m := \frac{p \cdot m_1 \cdot U_{1N}^2}{(4 \cdot \pi \cdot f_1) \cdot c_1 \cdot \left[ R_1 + \sqrt{R_1^2 + (X_1 + c_1 \cdot X'_2)^2} \right]} = 1.481 \times 10^3 \text{ J}$$

The torque units are N m but in mathcad is using J, so as we see  $J = N \cdot m = \text{Ws}$ .

154. Motor critical slip  $s_m$ :

$$s_m := \frac{c_1 \cdot R'_2}{\sqrt{R_1^2 + (X_1 + c_1 \cdot X'_2)^2}} = 0.10058$$

155. Factor a (Kloss):

$$a := \frac{2 \cdot R_1}{c_1 \cdot R'_2} = 3.736$$

156. Motor start torque  $M_p$ :

$$M_p := \frac{p \cdot m_1 \cdot U_{1N}^2 \cdot R'_2}{2 \cdot \pi \cdot f_1 \cdot \left[ (R_1 + c_1 \cdot R'_2)^2 + (X_1 + c_1 \cdot X'_2)^2 \right]} = 337.798$$

157. Motor dedicated torque  $M_N$ :

$$M_N := \frac{p \cdot P_{2N}}{2 \cdot \pi \cdot f_1 \cdot (1 - s_N)} = 534.687$$

158. Motor relative maximum torque  $m_m$ :

$$m_m := \frac{M_m}{M_N} = 2.771$$

\*Recommended value 2–3.2



159. Motor relative start torque  $m_p$ :

$$m_p := \frac{M_p}{M_N} = 0.632$$

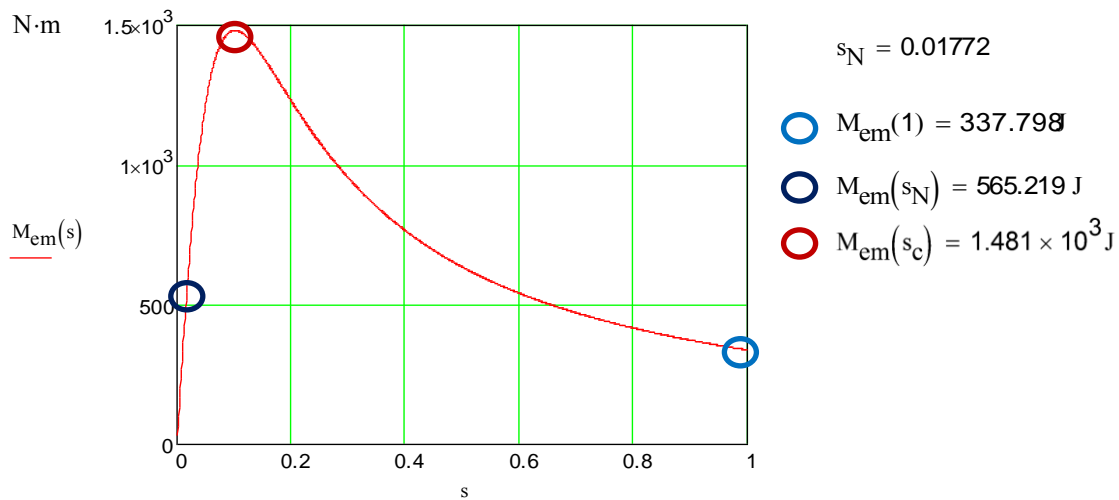
\*Recommended value accounting skin effect in rotor bars 0.7–2

\*Since we are not designing considering Skin-effect, the relative torque obtained is a bit lower than expected.

160. Motor mechanic characteristic:

$$\omega_1 := 2\pi \cdot f_1 = 314.159 \text{ s}^{-1} \quad s := 0.001, 0.002 \dots 1$$

$$M_{em}(s) := \frac{p \cdot m_1 \cdot U_{1N}^2 \cdot R'_2}{\omega_1 \cdot s \cdot \left[ \left( R_1 + c_1 \cdot \frac{R'_2}{s} \right)^2 + (X_1 + c_1 \cdot X'_2)^2 \right]}$$



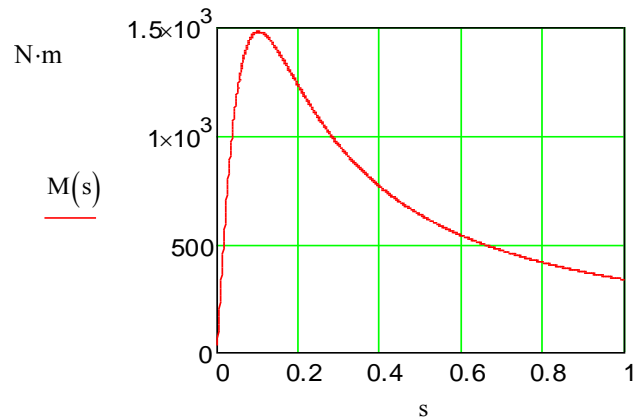
$$M_{em, vid} := \int_0^1 M_{em}(s) ds = 734.305 \quad M_{emvid} = 734.305 \text{ J}$$

$$s_c := \text{Maximize}(M_{em}, s) = 0.10058$$

161. Mechanical characteristic according to Kloss equation:

$$a = 3.736$$

$$M(s) := \frac{M_m \cdot (2 + a \cdot s_m)}{\frac{s_m}{s} + \frac{s}{s_m} + a \cdot s_m} \quad s_m := 0.001, 0.002 \dots 1$$



#### 4.1. Operating characteristics

162. Motor operating characteristics and dedicated parameters

$$P_{2N} = 55000 \text{ W}$$

$$U_{1N} = 80 \text{ V}$$

$$I_{1N} = 139.159 \text{ A}$$

$$P_{\text{Fea}} = 39.572 \text{ W}$$

$$R_1 = 19.301 \times 10^{-3} \Omega$$

$$c_1 = 1.014$$

$$P_{m\Sigma} = 417.401 \text{ W}$$

$$X_1 = 0.034 \Omega$$

$$X_m = 2.501 \Omega$$

$$R'_2 = 10.189 \times 10^{-3} \Omega$$

$$s_N = 0.01772$$

$$R_m = 0.116 \Omega$$

$$X'_2 = 0.066 \Omega$$

$$\eta_N := \eta$$

$$\eta_N = 0.92$$

$$s := 0.001, 0.005 \dots 1.5 \cdot s_N$$

$$Z_1 := R_1 + i \cdot X_1 = (0.019 + 0.034j) \Omega$$

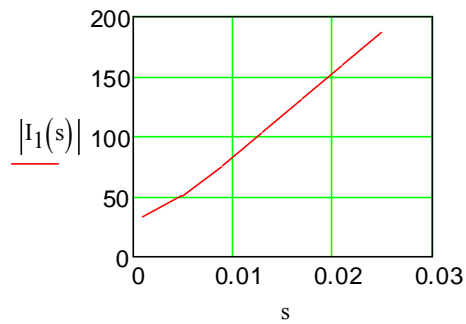
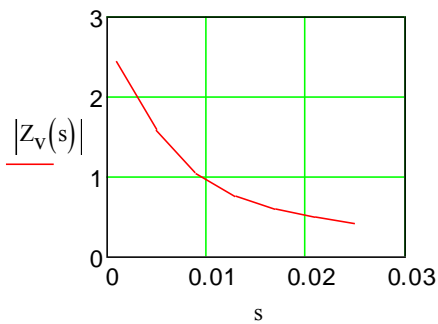
$$Z_m := R_m + i \cdot X_m = (0.116 + 2.501j) \Omega$$

$$Z_2(s) := \frac{R'_2}{s} + i \cdot X_2$$

$$Z_{2m}(s) := \frac{Z_m \cdot Z_2(s)}{Z_m + Z_2(s)}$$

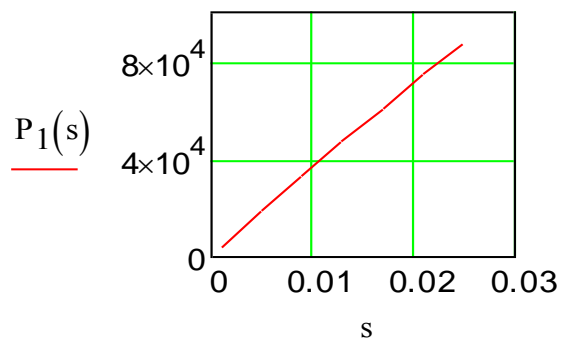
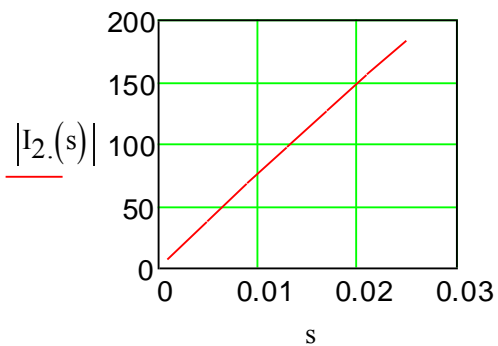
$$Z_v(s) := Z_1 + Z_{2m}(s)$$

$$I_1(s) := \frac{U_{1N}}{Z_v(s)}$$



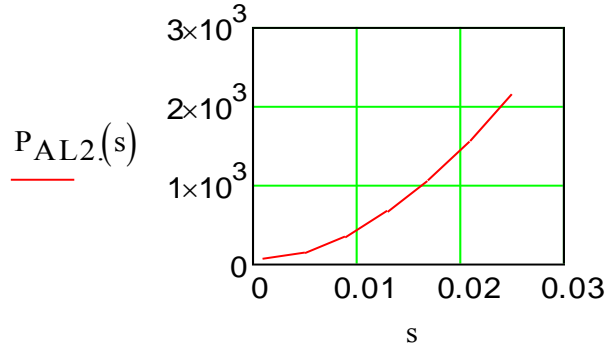
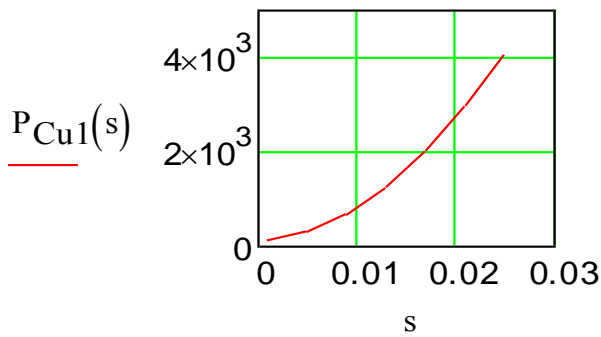
$$I_2(s) := I_1(s) \cdot \frac{Z_{2m}(s)}{Z_2(s)}$$

$$P_1(s) := m_1 \cdot U_{1N} \operatorname{Re}(I_1(s))$$



$$P_{Cu1}(s) := m_1 \cdot (|I_1(s)|)^2 \cdot R_1$$

$$P_{AL2}(s) := m_1 \cdot (|I_1(s)|)^2 \cdot R'_2$$



$$P_{1N} := \frac{P_{2N}}{\eta_N}$$

$$P_{pap}(s) := 0.005 P_{1N} \cdot \left( \frac{|I_1(s)|}{I_{1N}} \right)^2$$

$$P_{em}(s) := m_1 \cdot (|I_2(s)|)^2 \cdot \frac{R'_2}{s}$$

$$P_{0..} := P_{Feh} + P_{Fea} + P_{m\Sigma} = 1.15 \times 10^3 \text{ W}$$

$$M_N(s) := \frac{P \cdot P_{2N}}{2 \cdot \pi \cdot f_1 \cdot (1 - s_N)}$$

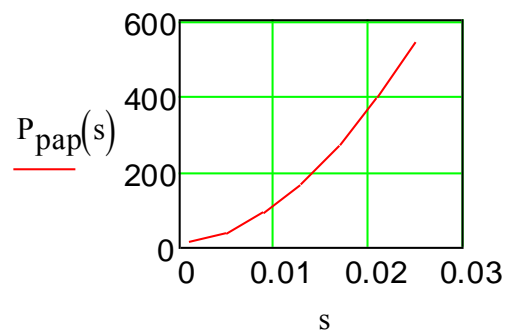
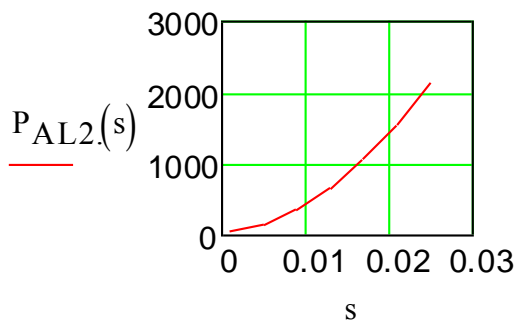
$$P_{\Sigma}(s) := P_{Cu1}(s) + P_{AL2}(s) + P_{0..} + P_{pap}(s)$$

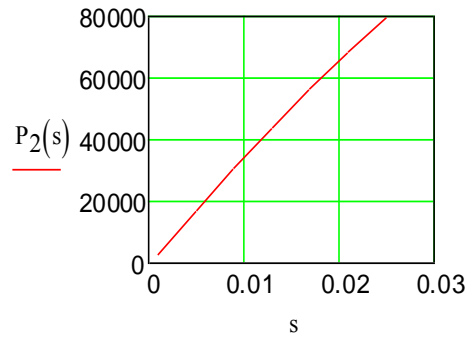
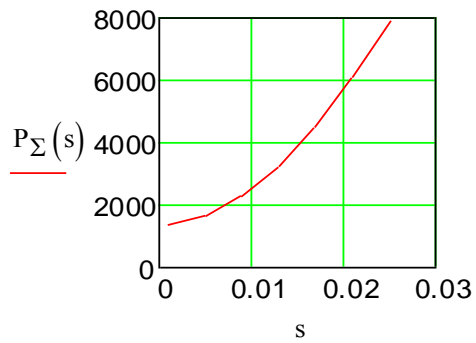
$$\eta(s) := 1 - \frac{P_{\Sigma}(s)}{P_1(s)}$$

$$\cos\phi(s) := \frac{\text{Re}(I_1(s))}{|I_1(s)|}$$

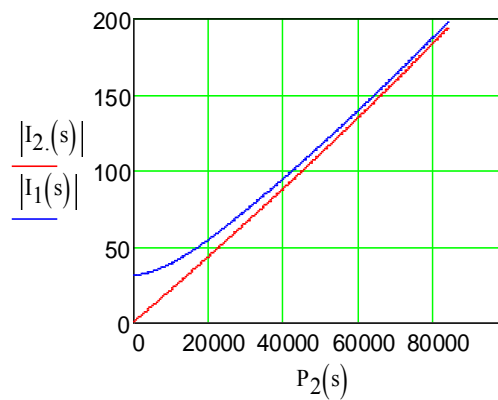
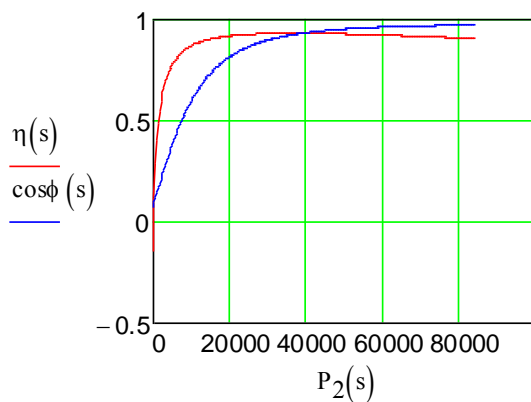
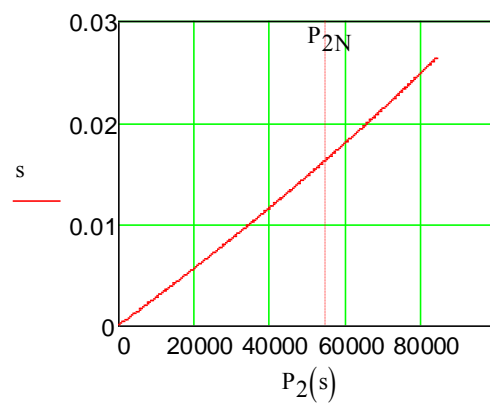
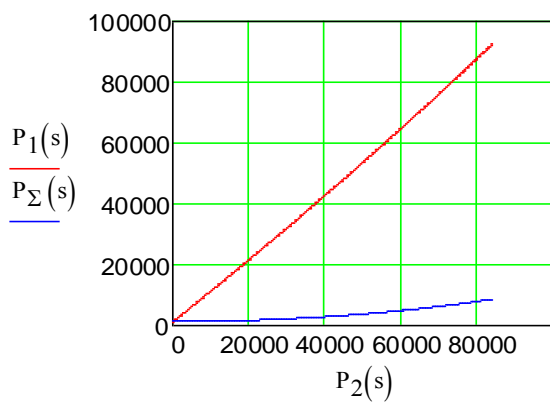
$$P_2(s) := P_1(s) - P_{\Sigma}(s)$$

$$M_{em}(s) := \frac{P \cdot P_{em}(s)}{2 \cdot \pi \cdot f_1}$$





$s := 0.0001, 0.0002 \dots 1.5 \cdot s_N$



Motor dedicated parameters:  $s := s_N$

$$P_{2N} = 55000 \text{ W}$$

$$U_{1N} = 80 \text{ V}$$

$$p = 3$$

$$s_N = 0.01772$$

$$\eta(s_N) = 0.925$$

$$|I_1(s_N)| = 137.489 \text{ A}$$

$$M_{N.}(s_N) = 534.687 \text{ J}$$

$$\cos\phi(s_N) = 0.963$$

$$|I_2(s_N)| = 132.651 \text{ A}$$

# Conclusions:

---

The potential advantages of multi-phase solutions over the conventional 3-phase ones make this kind of electrical machines especially interesting in applications where a reduction of the rotor harmonic losses, the power semiconductor stress of frequency regulator, higher torque, the torque pulsation reduction, capacity of response if one phase fail, etc. suppose the necessary difference for achieving efficiency and reliability goals. Speaking more about the characteristics reached with the model, it is important to remember that we are just taking in consideration the model for the first harmonic, even though we are reducing higher harmonic with the distribution factor. As the one of the biggest advantages, we must take special attention to the reduced relative magnetising current obtained (22.67 %) thanks to the great properties of this steel and its ratio quality/price making it an extremely attractive to the eyes of company and to the pocket of the customer. We also said that we did not made a deeper study in working conditions out of the steady state, concretely in the starting torque, when the vehicle is stopped and it might need a quick answer from the motor for the easy incorporation to the traffic, for example . I also mentioned that the skin effect of the slots was not really studied with a proper modelation, so in the late laboratory testing the real starting torque may be even higher than expected. In any case, the low starting torque is not supposing an inconvenient thanks to the frequency converter feeding the motor which is working with a very low pulsation in the beginning making constant area moment when the voltage proportional to the frequency, thereby increasing torque to maintain the constant size, keeping the power consumption low.

But probably the main goal or concern of this work was the capability to get a reliable and satisfying device with the lowest budget price. In this field it is especially relevant what we have been mentioning during all the work, the standardization of the components. Our model supposed a new breath of fresh air to the problems of the client, but with the components and models they are familiar in their daily activity with three phase induction motors. The decision of using common standards of three phase machines, give to the client the chance to keep working with their usual providers with the new design. This has two easy understandable advantages, the easy construction of the parts is a huge step to accelerate the insertation of the model in the market, and the price of developing these new parts is not going to suppose an increase on price. It is also important to remark that the duplication of electronic equipment for speed regulation of motor, is not supposing duplication in price. With the better distribution of the power through phases, the semiconductor component stress is lower and we can permit components with lower requirements of current, getting even a more competitive price thus we are using a less exigent technology.

Compared with probably the biggest competitor in vehicle motors, the synchronous machine with permanent magnets, even if the speed regulation of this one is much more comfortable, the price still

being a determinant factor in our favour since we are moving in a margin of price nearly similar to the three phase motor, and traditionally the price different between this two competitors is around 20% less for the asynchronous machine.

Anyway, as a final thought, it is important to discuss that the multi-phase machine technology still far to be completely investigated, and a lot of work still need to be done regarding to the improvement of models, speed regulation, losses, harmonics, etc

## Literature and Bibliography:

---

- ❖ *Electrical machines / Mikhail p. Kostenko and I. Piotrovsky, translated from the russian by a.e. Tchernukin,1977.*
  
- ❖ *Asinchroniniu narveliniu varikliu ekvivalentines schemos parametru ir charaktesirtiku skaiciavimas,KTU,electrical system katedra.*
  
- ❖ *Power system stability and control, by Prabha Kundur,1994.*
  
- ❖ *Article:weg explains how reducing efficiency losses is key to achieving ie4 class efficiency with induction motors.*
  
- ❖ *Realization of an asynchronous six-phase induction motor drive test-rig,by r. Gregor, f. Barrero, s. Toral and m.j. Durán, e.s.i., university of seville.*
  
- ❖ *Design, development of six phase squirrel cage induction motor and its comparative analysis with equivalent three phase squirrel cage induction motor using circle diagram, international journal of emerging technology and advanced engineering*



- ❖ *Research of six-phase induction motor windings, by b. Kundrotas, a. Petrovas, r. Rinkeviciene, a. Smilgevicius, department of automation, vilnius gediminas technical university*
- ❖ *Analysis on the mathematical model of the six-phase induction motor of the electric vehicle, by chaoyong tuo, hunan mechanic & electric polytechnic, changsha*
- ❖ *Multiphase induction motor drives - a technology Status review, by e. Levi, r. Bojoi, f. Profumo, h.a. Toliyat and s. Williamson.*
- ❖ *Status review, by e. Levi, r. Bojoi, f. Profumo, h.a. Toliyat and s. Williamson.*
- ❖ *The state of the art of electric and hybrid Vehicles, by c. C. Chan, fellow, ieee*
- ❖ *High phase order induction motors part i-description and theoretical considerations, e.a. Klingshirn, senior member, ieee*
- ❖ *Skin Effect in Squirrel Cage Rotor Bars and Its Consideration in Simulation of Non-steady-state Operation of Induction Machines, by Marcel Benecke, Reinhard Doebbelin, Gerd Griepentrog, and Andreas Lindemann*
- ❖ *IEC website resources, <http://www.iec.ch/>*
- ❖ *ABB website resources, <http://www.abb.com/>*
- ❖ *Siemens website resources, <http://www.siemens.com/entry/cc/en/>*



# Appendix:

**P.1 lentelė.** Variklių nominaliosios naudingosios galios  $P_{2N}$  priklausomybė nuo sukimosi ašies aukščio  $h$

$h, 10^{-3}\text{m}$	$P_{2N}, \text{W, kai}$			
	$2p=2$	$2p=4$	$2p=6$	$2p=8$
50	90	60	-	-
	120	90	-	-
56	180	120	-	-
	250	180	-	-
63	370	250	180	-
	550	370	250	-
71	750	550	370	250
	1100	750	550	-
80	1500	1100	750	370
	2200	1500	1100	550
90	3000	2200	1500	750
	-	-	-	1100
100	4000	3000	-	-
	5500	4000	2200	1500
112	7500	5500	3000	2200
	-	-	4000	3000
132	-	7500	5500	4000
	11000	11000	7500	5500
160	15000	15000	11000	7500
	18500	18500	15000	11000
180	22000	22000	-	-
	30000	30000	18500	15000
200	37000	37000	22000	18500
	45000	45000	30000	22000
225	55000	55000	37000	30000
250	75000	75000	45000	37000
	90000	90000	55000	45000

**P.2 lentelė.** Išoriniai statoriaus skersmenys ir juos atitinkantys elektrotechninio plieno juostų, iš kurių šampuojami magnetolaidžių lakštai, pločiai  $b_j$

$h, 10^{-3} \text{m}$	$h'_2, 10^{-3} \text{m}$	$D_{j1 \max}, 10^{-3} \text{m}$	$b_j, 10^{-3} \text{m}$
50	7,0	86 (81)	90
56	8,0	96 (89)	100
63	9,0	108 (100)	113
71	10,0	122 (116)	127
80	10,5	139 (131)	145
90	11,5	157 (149)	163
100	12,5	175 (168)	182
112	13,5	197 (191)	204
132	15,5	233 (225)	240
160	17,5	285 (272)	292
180	19,0	322 (313)	330
200	20,5	359 (349)	367
225	22,5	406 (392)	414
250	24,0	452 (437)	460

Skliausteliuose pateikti 4A serijos variklių statorių magnetolaidžių skersmenys

**P.3 lentelė.** Rekomenduojamos  $q_1$  reikšmės

$h, 10^{-3} \text{m}$	$q_1, \text{kai}$			
	$2p=2$	$2p=4$	$2p=6$	$2p=8$
50-63	4	2	2	-
71	4	2	2	1,5
80-100	4	3	2	1,5
112-132	4	3	3	2
160	6	4	3	2
180-225	6	4	4	3
250	8	5	4	3

**P.4 lentelė.** Statoriaus dvivluoksnės apvijos faktorių  $k_{d01}$ ,  $k_{\beta 1}$ ,  $k_{w1}=f(q_1)$  reikšmės

$q_1$	$k_{d01}$	$\frac{Z_1}{2p}$	$2p=2$				$2p \geq 4$			
			$y_{n1}$	$\beta$	$k_{\beta 1}$	$k_{w1}$	$y_{n1}$	$\beta$	$k_{\beta 1}$	$k_{w1}$
1,5	0,965	4,5	-	-	-	-	4	0,980	0,985	0,960
2	0,966	6	-	-	-	-	5	0,833	0,966	0,935
2,5	0,962	7,5	-	-	-	-	6	0,800	0,951	0,915
3	0,960	9	-	-	-	-	7	0,778	0,94	0,905
4	0,958	12	-	-	-	-	10	0,833	0,966	0,925
5	0,957	15	-	-	-	-	12	0,800	0,951	0,911
6	0,957	18	11	0,610	0,818	0,785	15	0,833	0,966	0,925
8	0,956	24	15	0,625	0,832	0,795	19	0,792	0,947	0,905

**P.5 lentelė.** Apvalių varinių emaliuotų laidų skersmenys ir skerspjūvio plotai

Neizoliuoto laido nominalus skersmuo $d, 10^{-3}\text{m}$	Vidutinis izoliuoto laido skersmuo $d_i, 10^{-3}\text{m}$	Neizoliuoto laido skerspjūvio plotas $q, 10^{-6}\text{m}^2$	Neizoliuoto laido nominalus skersmuo $d, 10^{-3}\text{m}$	Vidutinis izoliuoto laido skersmuo $d_i, 10^{-3}\text{m}$	Neizoliuoto laido skerspjūvio plotas $q, 10^{-6}\text{m}^2$
0,23	0,265	0,0415	0,75	0,815	0,442
0,25	0,285	0,0491	0,77	0,835	0,466
0,27	0,305	0,0573	0,80	0,865	0,503
0,28	0,315	0,0616	0,83	0,895	0,541
0,29	0,325	0,0661	0,85	0,915	0,567
0,31	0,345	0,0755	0,86	0,925	0,581
0,33	0,365	0,0655	0,90	0,965	0,636
0,35	0,390	0,0962	0,93	0,995	0,679
0,38	0,420	0,1134	0,95	1,015	0,709
0,40	0,440	0,1257	0,96	1,025	0,724
0,41	0,450	0,1320	1,00	1,080	0,785
0,44	0,480	0,1521	1,04	1,120	0,849
0,45	0,490	0,1590	1,06	1,140	0,883
0,47	0,510	0,1735	1,08	1,160	0,916
0,49	0,530	0,1886	1,12	1,200	0,985
0,50	0,545	0,1963	1,16	1,240	1,057
0,51	0,565	0,204	1,18	1,260	1,094
0,53	0,585	0,221	1,20	1,280	1,131
0,55	0,605	0,238	1,25	1,330	1,227
0,56	0,615	0,246	1,30	1,385	1,327
0,57	0,625	0,255	1,32	1,405	1,366
0,59	0,645	0,273	1,35	1,435	1,431
0,62	0,675	0,302	1,40	1,485	1,539
0,63	0,690	0,312	1,45	1,535	1,651
0,64	0,700	0,322	1,50	1,585	1,767
0,67	0,730	0,353	1,56	1,645	1,911
0,69	0,750	0,374	1,60	1,685	2,011
0,71	0,770	0,396	1,62	1,705	2,060
0,72	0,780	0,407	1,68	1,765	2,220
0,74	0,805	0,430	1,70	1,785	2,270

**P.6 lentelė.** Santykinės  $A_1 \cdot J_1$  vertės priklausomai nuo izoliacijos klasės

$h, 10^{-3}\text{m}$	Rekomenduojama izoliacijos klasė	Santytinės $A_1 \cdot J_1$ vertės, kai izoliacijos klasė		
		B	F	H
50-132	B	1,0	1,33	1,75
$\geq 160$	F	0,75	1,0	1,30

**P.7 lentelė.** Vidutinės statoriaus jungų magnetinių srautų tankių vertės

$h, 10^{-3} \text{m}$	$U, \text{V}$	$2p$	Jungo magnetinio srauto tankis $B_{j1}, \text{T}$
50-132	$\leq 660$	2;4	1,35-1,65
		6	1,30-1,60
		8	1,05-1,35
160-250	$\leq 660$	2;4	1,30-1,60
		6	1,20-1,50
		8	1,00-1,20

**Pastaba.** Rekomenduojama priimti vidutinę aritmetinę  $B_{j1}$  vertę

**P.8 lentelė.** Vidutinės statoriaus dantų magnetinių srautų tankių vertės

$h, 10^{-3} \text{m}$	$U, \text{V}$	$2p$	Danties magnetinio srauto tankis $B_{z1}, \text{T}$
50-132	$\leq 660$	2;4;6	1,60-1,90
		8	1,55-1,65
160-250	$\leq 660$	2	1,60-1,90
		4;6;8	1,55-1,80

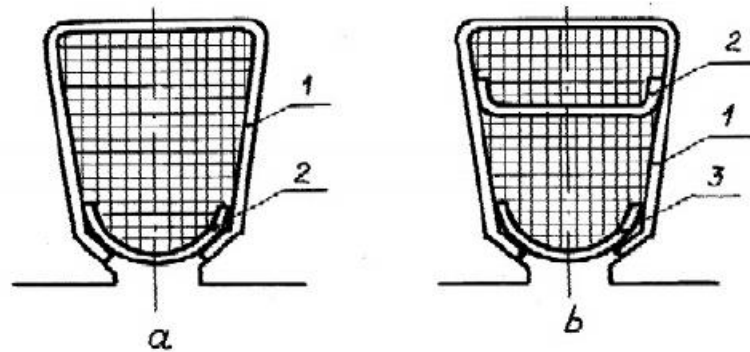
**Pastaba.** Rekomenduojama parinkti vidutinę aritmetinę  $B_{z1}$  vertę

**P.9 lentelė.** Statoriaus pusiau uždaro griovelio vidutinės prapjovos pločio vertės

$h, 10^{-3} \text{m}$	$b_{\text{gr}}, 10^{-3} \text{m}, \text{ kai}$			
	$2p=2$	$2p=4$	$2p=6$	$2p=8$
50-63	1,8	1,8	1,8	1,8
71	2,0	2,0	2,0	2,0
80, 90	3,0	3,0	2,7	2,7
100, 112	3,5	3,5	3,0	3,0
132	4,0	3,5	3,5	3,5
160-250	4,0	3,7	3,7	3,7

**P.10 lentelė.** Statoriaus ir rotoriaus griovelių matmenų užlaidos, atsižvelgiant į magnetolaidžių surinkimo paklaidas

$h, 10^{-3} \text{m}$	Užlaidos, $10^{-3} \text{m}$	
	pagal plotį, $\Delta b_{\text{gr}}$	pagal griovelio aukštį, $\Delta h_{\text{gr}}$
50-132	0,1	0,1
160-250	0,2	0,2



P.1 11 lentelė. Asinchroninių variklių statoriaus apvijų griovelio izoliacija

Apvija	Sukimosi ašies aukštis $h$ , $10^{-3}$ m	Pozicija	Medžiagos pavadinimas		Medžiagos storis, $10^{-3}$ m	Stuoksnų skaičius	Izoliacijos storis $b_i$ , $10^{-3}$ m
			B klasė	F, H klasė			
Viensluoksnė a pav.	50-80	1	Izofleksinė stiklo plėvelė	Imidofleksinė stiklo plėvelė	0,2	1	0,2
		2	Tas pats	Tas pats	0,3	1	0,3
	90-132	1	Izofleksinė stiklo plėvelė	Imidofleksinė stiklo plėvelė	0,25	1	0,25
		2	Tas pats	Tas pats	0,35	1	0,35
Dvisluoksnė b pav.	160-250	1	Izofleksinė stiklo plėvelė	Imidofleksinė stiklo plėvelė	0,4	1	0,4
		2	Tas pats	Tas pats	0,4	1	0,4
		3	Tas pats	Tas pats	0,5	1	0,5

**Pastaba.** Tarpfazinei apvijų galūnių izoliacijai naudojama medžiaga nurodyta 1 pozicijoje

P.12 lentelė. Statoriaus griovelio izoliacijos storio  $b_i$  vertės

$h$ , $10^{-3}$ m	$b_i$ , $10^{-3}$ m, kai izoliacijos klasė		
	B	F	H
50-80	0,20	0,20	0,20
90-132	0,25	0,25	0,25
160-250	0,40	0,40	0,40



**P.13 lentelė.** Statoriaus griovelio tarpsluoksninės ir uždarnosios izoliacijos skerspjūvio ploto  $Q_i$  vertės

$h, 10^{-3}\text{m}$	Apvijos tipas	$Q_i, \text{m}^2$
50-132	Viensluoksnė	$0,5 b_2 10^{-3}$
160-250	Dvisluoksnė	$0,4 b_1 10^{-3} + 0,9 b_2 10^{-3}$

**P.14 lentelė.** Rekomenduojami asinchroninių variklių su narveliniu rotoriumi statoriaus ir rotoriaus magnetolaidžių griovelių skaičiai

$h, 10^{-3}\text{m}$	$Z_1/Z_2, \text{kai}$			
	$2p=2$	$2p=4$	$2p=6$	$2p=8$
50-63	24/19	24/18	36/28	–
71	24/19	24/18	36/28	36/28
80-100	24/19	36/28	36/28	36/28
112-132	24/19	36/34	54/51	48/44
160	36/28	48/38	54/51	48/44
180-200	36/28	48/38	72/58	72/58
225	36/28	48/38	72/56	72/56
250	48/40	60/50	72/56	72/56

**P.16 lentelė.** Rotoriaus jungų leidžiami didžiausieji magnetinio srauto tankiai

Didžiausias rotoriaus jungo magnetinio srauto tankis $B_{j2}, \text{T}, \text{kai}$			
$2p=2$	$2p=4$	$2p=6$	$2p=8$
1,45	1,25	1,15	0,85

**P.17 lentelė.** 2013 markės elektrotechninio plieno pagrindinė įmagnetinimo charakteristika

$B, T$	0,00	0,01	0,02	0,03	0,04	0,05	0,06	0,07	0,08	0,09
	$H, 10^2 A/m$									
0,4	0,56	0,56	0,57	0,58	0,59	0,60	0,60	0,61	0,61	0,62
0,5	0,63	0,63	0,64	0,65	0,66	0,67	0,67	0,66	0,68	0,69
0,6	0,70	0,70	0,71	0,72	0,73	0,74	0,74	0,75	0,76	0,77
0,7	0,78	0,79	0,80	0,81	0,82	0,83	0,84	0,85	0,86	0,87
0,8	0,88	0,89	0,90	0,91	0,92	0,93	0,94	0,95	0,96	0,97
0,9	0,99	1,00	1,01	1,02	1,03	1,04	1,05	1,06	1,07	1,08
1,0	1,10	1,11	1,13	1,14	1,15	1,17	1,18	1,20	1,21	1,23
1,1	1,25	1,26	1,27	1,28	1,29	1,32	1,33	1,34	1,36	1,38
1,2	1,41	1,46	1,52	1,58	1,64	1,70	1,76	1,82	1,88	1,94
1,3	2,00	2,10	2,20	2,30	2,40	2,50	2,60	2,70	2,80	2,90
1,4	3,00	3,20	3,50	3,80	4,10	4,30	4,60	5,00	5,40	5,80
1,5	6,20	6,70	7,80	8,90	10,0	11,3	12,4	13,5	14,6	15,8
1,6	17,0	18,6	20,2	21,8	23,4	25,0	27,0	28,0	30,0	32,0
1,7	34,0	37,0	40,0	43,0	47,0	50,0	54,0	58,0	62,0	66,0
1,8	70,0	75,0	80,0	85,0	92,0	100	106	112	118	124
1,9	130	136	142	148	156	165	173	181	189	198
2,0	207	226	244	263	281	300	360	420	480	540
2,1	600	670	740	820	880	950	1020	1090	1160	1230
2,2	1300	1380	1460	1540	1620	1700	1780	1860	1940	2020
2,3	2100	2180	2260	2340	2420	2500	2580	2660	2740	2820
2,4	2900	2980	3060	3140	3220	3300	3380	3460	3540	3620

**P.19 lentelė.** Faktorius  $k_{q1}$  reikšmės

$q_1$	Faktorius $k_{q1}$ , kai						
	$\frac{Z_2}{p} = 10$	$\frac{Z_2}{p} = 15$	$\frac{Z_2}{p} = 20$	$\frac{Z_2}{p} = 25$	$\frac{Z_2}{p} = 30$	$\frac{Z_2}{p} = 35$	$\frac{Z_2}{p} = 40$
2	$\frac{0,99}{0,94}$	$\frac{0,94}{0,87}$	$\frac{0,87}{0,77}$	–	–	–	–
3	$\frac{0,98}{0,92}$	$\frac{0,93}{0,87}$	$\frac{0,88}{0,84}$	$\frac{0,85}{0,78}$	$\frac{0,81}{0,68}$	–	–
4	$\frac{0,97}{0,90}$	$\frac{0,90}{0,81}$	$\frac{0,84}{0,77}$	$\frac{0,80}{0,75}$	$\frac{0,77}{0,72}$	$\frac{0,74}{0,67}$	–
5	–	$\frac{0,86}{0,78}$	$\frac{0,81}{0,71}$	$\frac{0,75}{0,69}$	$\frac{0,72}{0,67}$	$\frac{0,70}{0,65}$	$\frac{0,67}{0,62}$
6	–	$\frac{0,82}{0,73}$	$\frac{0,74}{0,67}$	$\frac{0,70}{0,62}$	$\frac{0,66}{0,60}$	$\frac{0,62}{0,58}$	$\frac{0,61}{0,57}$
8	–	$\frac{0,78}{0,66}$	$\frac{0,67}{0,56}$	$\frac{0,60}{0,52}$	$\frac{0,56}{0,49}$	$\frac{0,53}{0,47}$	$\frac{0,51}{0,46}$

**Pastaba.** Skaitiklyje nurodytos faktorius  $k_{q1}$  reikšmės varikliams su įstrižais grioveliais ( $b_s \approx t_1$ ), o vardiklyje – varikliams su tiesiais grioveliais.

**P.20 lentelė.** Faktorius  $k'_{d1}$  reikšmės

$k_{y1}$	Faktorius $k'_{d1}$ , kai							
	$q_1=1$	$q_1=2$	$q_1=3$	$q_1=4$	$q_1=5$	$q_1=6$	$q_1=7$	$q_1=8$
0	0,097	0,0285	0,0141	0,0089	0,0065	0,0052	0,0044	0,0039
1	0,097	0,0235	0,0115	0,0074	0,0053	0,0045	0,0037	0,0033
2		0,0285	0,0111	0,0062	0,0044	0,0036	0,0032	0,0026
3		0,0270	0,0141	0,0069	0,0043	0,0030	0,0029	0,0023
4			0,0138	0,0089	0,0055	0,0031	0,0025	0,0019
5				0,0066	0,0065	0,0042	0,0031	0,0021
6					0,0063	0,0052	0,0032	0,0026
7					0,0060	0,0052	0,0040	0,0032
8						0,0055	0,0042	0,0039
9							0,0044	0,0044
10								0,0045

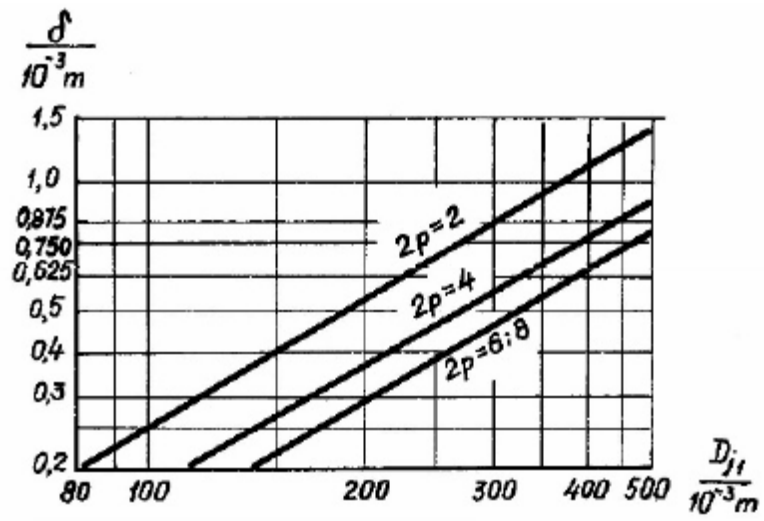
**Pastaba.** Apvijos žingsnio sutrumpinimas, išreikštas griovelių skaičiumi,  $k_{y1} = \tau \cdot y_{n1}$ ,

čia  $\tau = \frac{Z_1}{2p}$ ,  $y_{n1} = \beta \tau$ . Viensluksnei pilnojo žingsnio apvijai  $k_{y1} = 0$ . Kai  $q_1 = 1,5$  ir  $\beta = 0,89$ ,

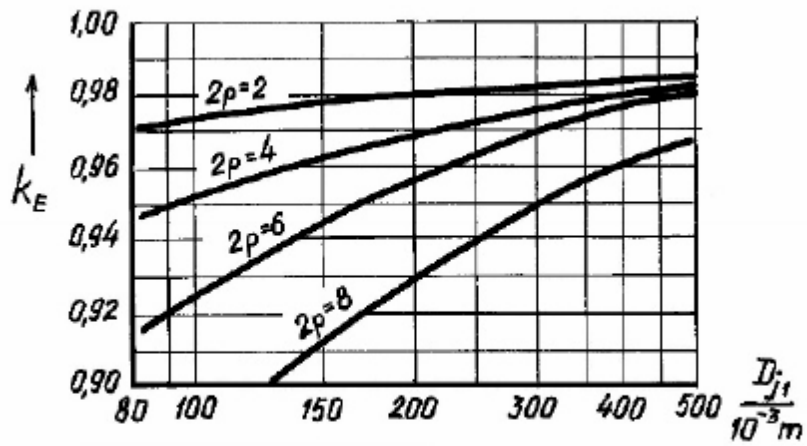
tai  $k'_{d1} = 0,045$ , o kai  $q_1 = 2,5$  ir  $\beta = 0,80$ ,  $k'_{d1} = 0,017$ .

**P.21 lentelė.** Faktorius  $k_\varepsilon$  reikšmės

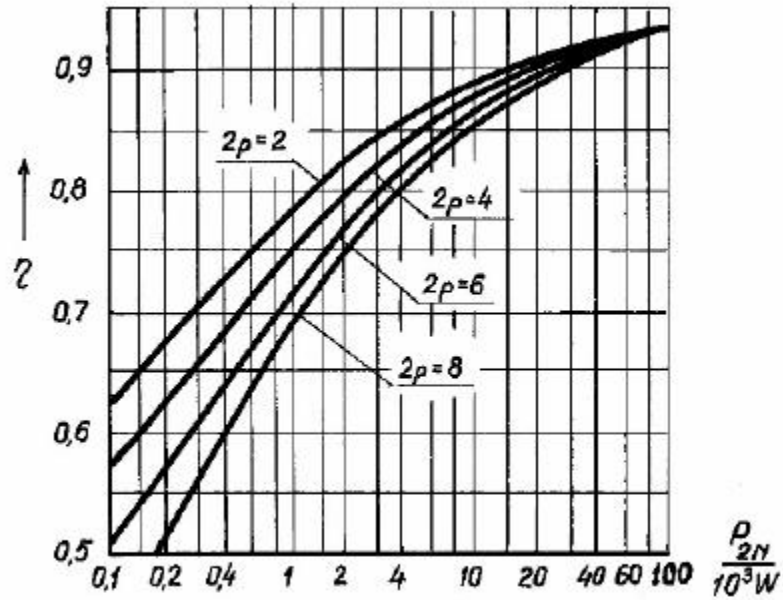
$y_s$ , rad	Faktorius $k_\varepsilon$ , kai											
	$\varepsilon=15$	$\varepsilon=20$	$\varepsilon=25$	$\varepsilon=30$	$\varepsilon=35$	$\varepsilon=40$	$\varepsilon=45$	$\varepsilon=50$	$\varepsilon=55$	$\varepsilon=60$	$\varepsilon=65$	$\varepsilon=70$
0,174	1,0177	1,0240	1,031	1,036	1,043	1,049	1,055	1,062	1,068	1,074	1,081	1,087
0,208	1,0256	1,0347	1,044	1,053	1,062	1,071	1,080	1,088	1,098	1,107	1,117	1,126
0,244	1,0347	1,0471	1,059	1,072	1,084	1,097	1,109	1,122	1,134	1,146	1,159	1,171
0,280	1,045	1,061	1,078	1,094	1,100	1,126	1,142	1,159	1,175	1,192	1,207	1,223
0,348	1,070	1,096	1,121	1,146	1,172	1,197	1,222	1,247	1,273	1,298	1,324	1,348
0,435	1,100	1,149	1,189	1,280	1,267	1,307	1,346	1,385	1,424	1,463	1,501	1,540
0,522	1,159	1,216	1,273	1,330	1,387	1,444	1,500	1,558	1,615	1,671	1,73	1,786
0,696	1,357	1,485	1,612	1,740	1,868	1,990	2,12	2,25	2,38	2,505	2,63	2,760
0,870	1,745	2,01	2,27	2,54	2,81	3,07	3,34	3,60	3,87	4,14	4,40	4,660
1,044	2,15	2,56	2,97	3,38	3,80	4,20	4,62	5,03	5,44	5,85	6,25	6,666



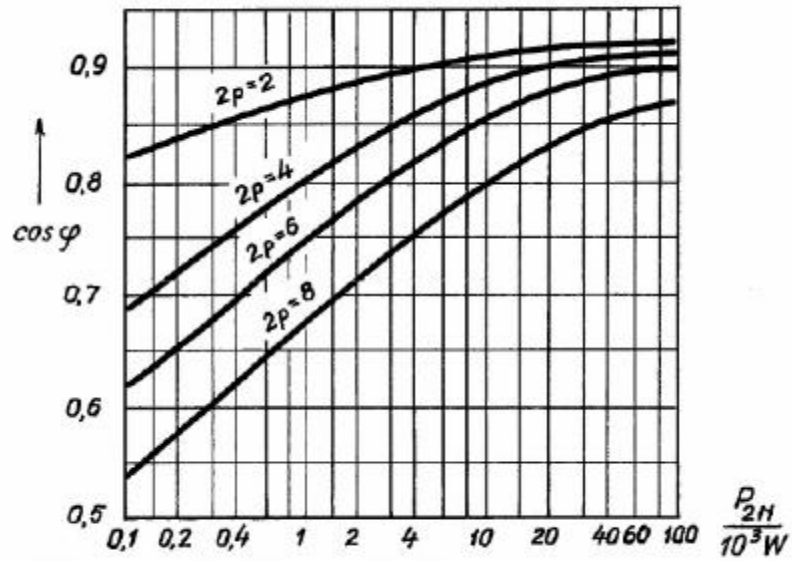
P.2 pav. Vidutinės  $\delta = f(D_{j1})$  vertės



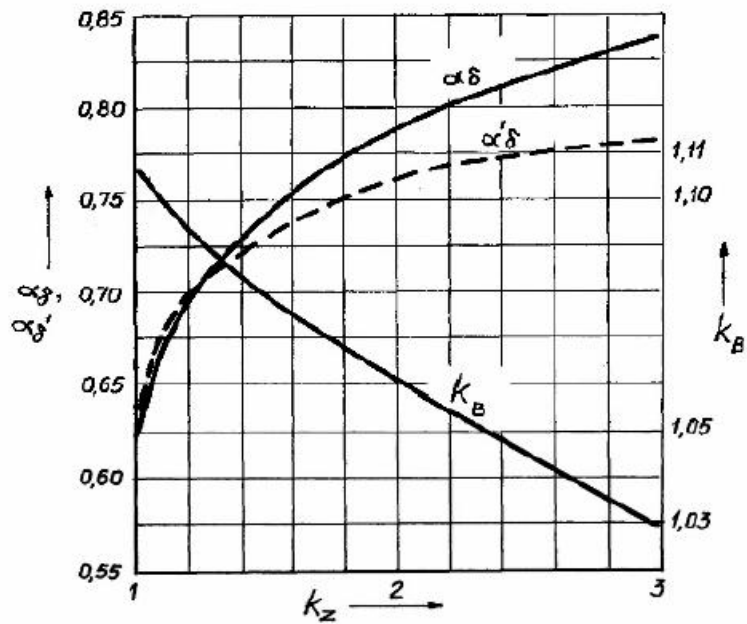
P.3 pav. Vidutinės  $k_E = f(D_{j1})$  vertės



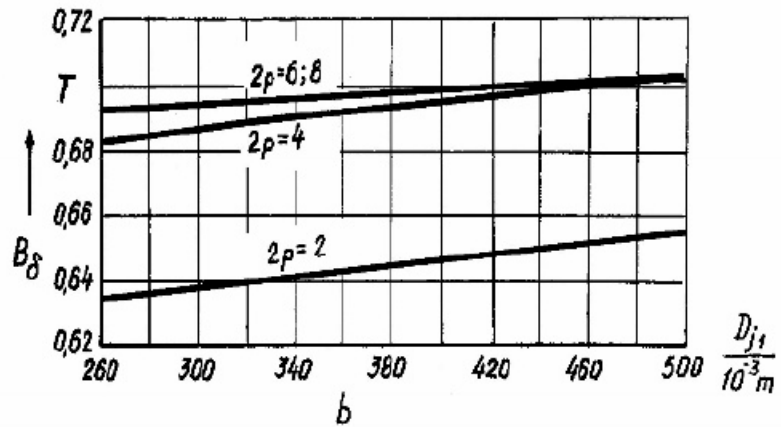
P.4 pav. Vidutinės  $\eta = f(P_{2N})$  vertės



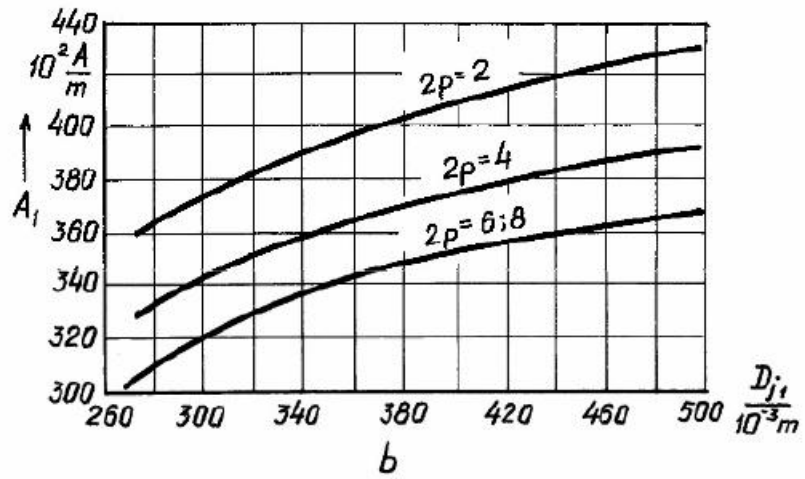
P.5 pav. Vidutinės  $\cos \varphi = f(P_{2N})$  vertės



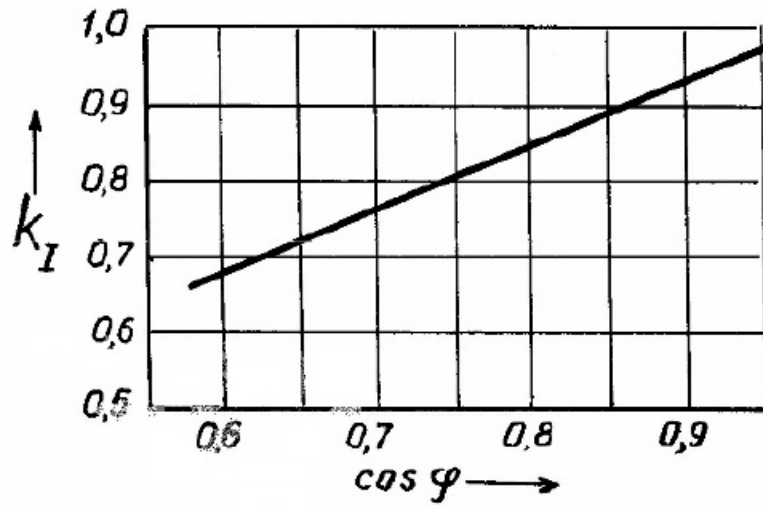
P.6 pav. Faktorių  $\alpha_\delta$ ,  $\alpha'_\delta$ ,  $k_B = f(k_z)$  vertės



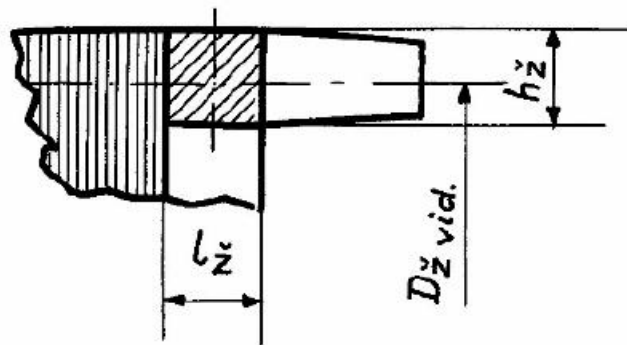
P.7 pav. Vidutinės  $B_\delta = f(D_{j1})$  vertės



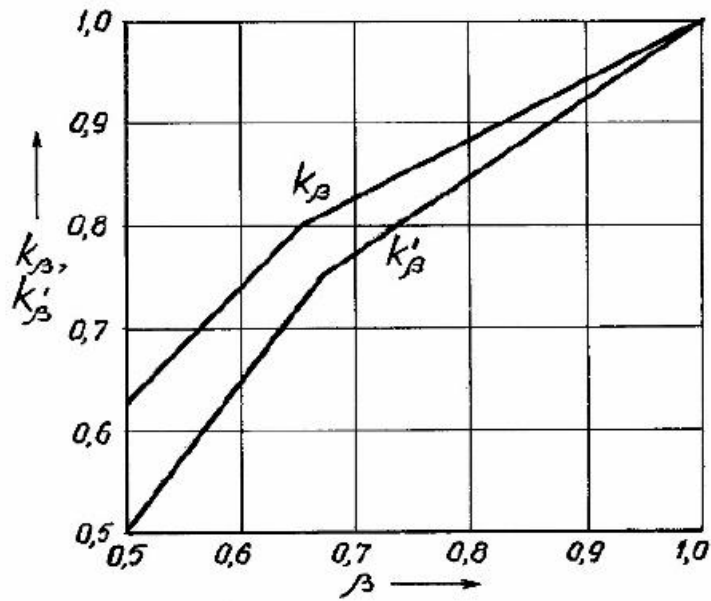
P.8 pav. Vidutinės  $A_1 = f(D_{j1})$  vertės



P.18 pav. Faktorius  $k_1 = f(\cos \varphi)$  vertės

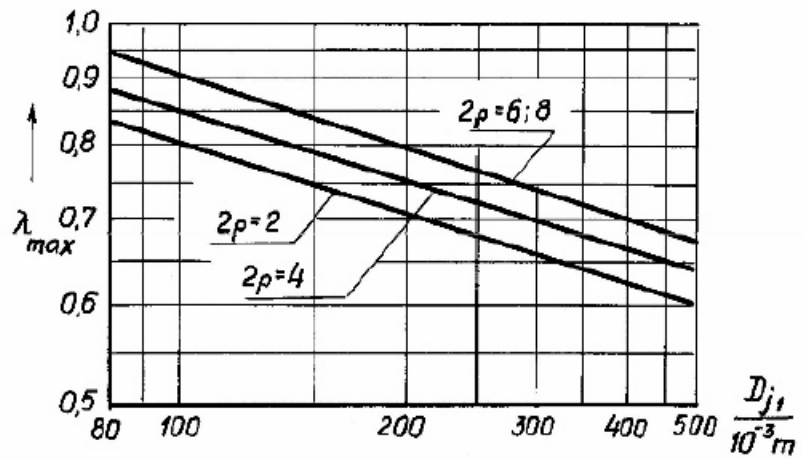


P.19 pav. Narvelinio rotoriaus žiedo matmenys

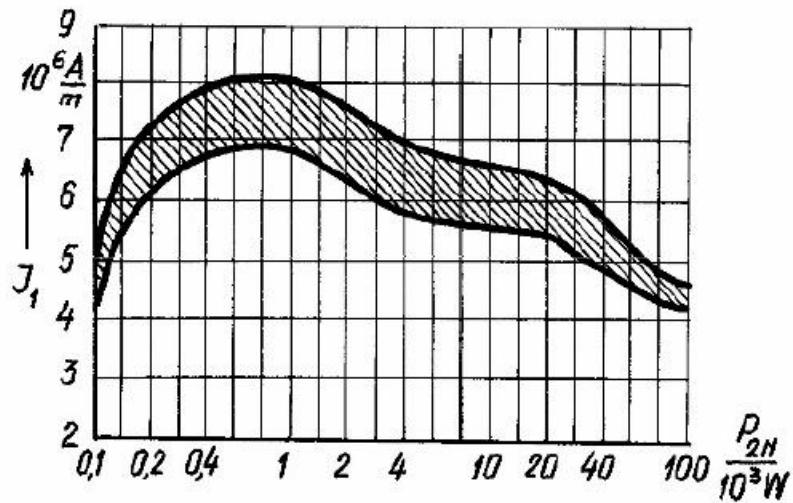


P.21 pav. Faktoriai  $k_\beta$  ir  $k'_\beta = f(\beta)$

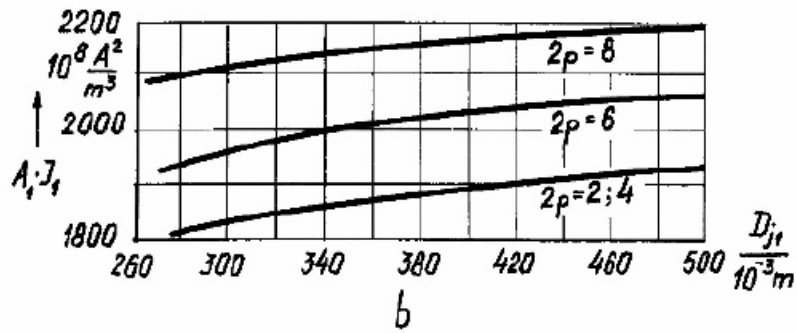




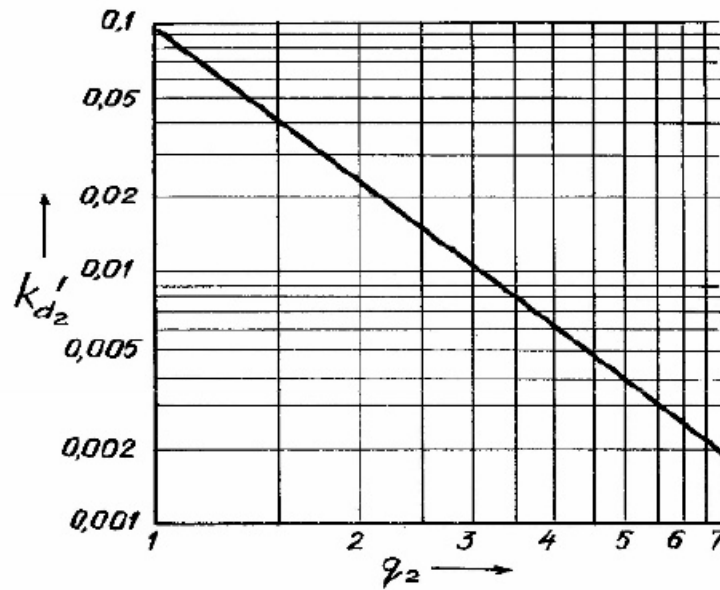
P.9 pav. Ribinès  $\lambda_{max} = f(D_{j1})$  vertės



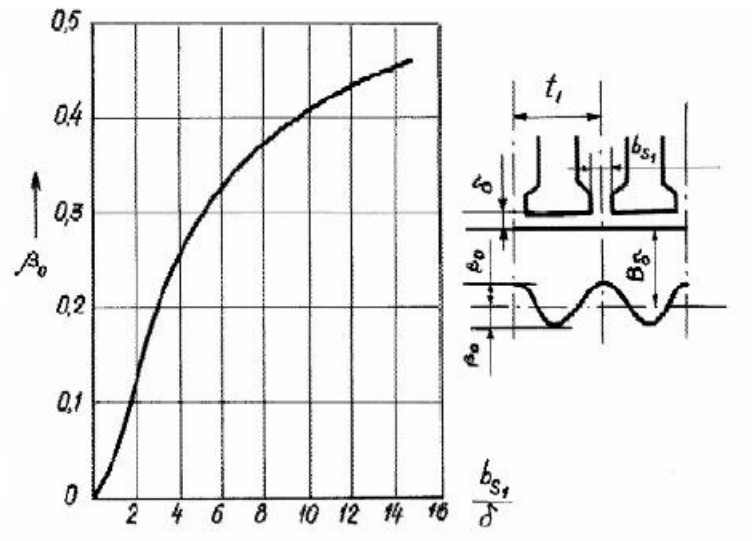
P.12 pav. Srovės tankio  $J_1$  kitimo ribos



P.13 pav. Vidutinės  $A_1 J_1 = f(D_{j1})$  vertės



P.22 pav. Faktorius  $k_{d2}' = f(q_2)$ , kai  $q_2 = \frac{Z_2}{2pm_1}$ ;



P.23 pav. Faktorius  $\beta_0 = f(b_{s1}/\delta)$